

Introduction to Nuclear Fusion

Prof. Dr. Yong-Su Na

Plasma transport in a Tokamak

Tokamak Transport

- Transport in fusion plasmas is 'anomalous'.

- Normal (water) flow: Hydrodynamic equations can develop nonlinear turbulent solutions (Reynolds, 1883)

$$\text{Re} = \frac{\text{inertial forces}}{\text{viscous forces}} = \frac{\rho v L}{\mu} = \frac{v L}{\nu}$$

ρ : density of the fluid (kg/m³)

v : mean velocity of the object relative to the fluid (m/s)

L : a characteristic linear dimension, (travelled length of the fluid; hydraulic diameter when dealing with river systems) (m)

μ : dynamic viscosity of the fluid (Pa·s or N·s/m² or kg/(m·s))

ν : kinematic viscosity (μ/ρ) (m²/s)

Tokamak Transport

- Transport in fusion plasmas is 'anomalous'.

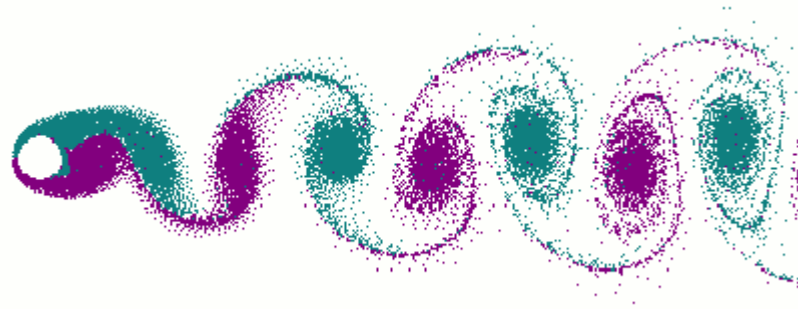
- Normal (water) flow: Hydrodynamic equations can develop nonlinear turbulent solutions (Reynolds, 1883)

$$\text{Re} = \frac{\text{diffusion time scale}}{\text{advection time scale}} = \frac{v/L}{v/L^2} = \frac{t_d}{t_a}$$

v : mean velocity of the object relative to the fluid (m/s)

L : a characteristic linear dimension, (travelled length of the fluid; hydraulic diameter when dealing with river systems) (m)

ν : kinematic viscosity (μ/ρ) (m²/s)



A vortex street around a cylinder. This occurs around cylinders, for any fluid, cylinder size and fluid speed, provided that there is a Reynolds number of between ~ 40 and 10^3 . Cf. In a pipe water flow, transition from laminar to turbulent flow around $\text{Re} \sim 2300$.



Tokamak Transport

- **Transport in fusion plasmas is 'anomalous'.**

- Normal (water) flow: Hydrodynamic equations can develop nonlinear turbulent solutions (Reynolds, 1883)

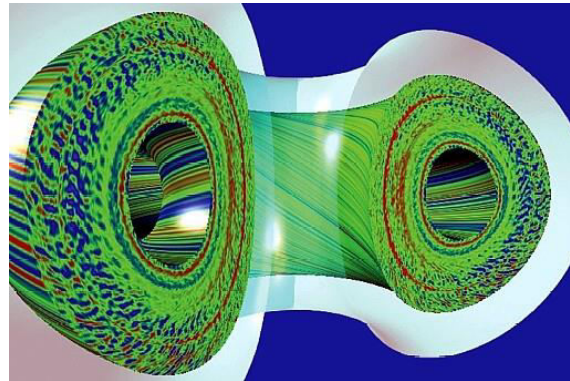
*"When I meet God, I am going to ask him two questions:
Why relativity? And why turbulence?
I really believe he will have an answer for the first."*

- Werner Heisenberg

Tokamak Transport

- Transport in fusion plasmas is 'anomalous'.

- Normal (water) flow: Hydrodynamic equations can develop nonlinear turbulent solutions (Reynolds, 1883)
- Transport mainly governed by turbulence:
 - radial extent of turbulent eddy: 1 - 2 cm
 - typical lifetime of turbulent eddy: 0.5 - 1 ms



- Classical
 - $\chi_i \sim 40\chi_e$
 - $\sim 10^{-4} \text{ m}^2/\text{s}$

Bohm diffusion (1946):

$$D_{\perp} = \frac{1}{16} \frac{kT_e}{eB}$$

- Anomalous transport coefficients are of the order $1 \text{ m}^2/\text{s}$

$$D \sim \frac{(\Delta x)^2}{\tau} : \text{diffusion coefficient (m}^2/\text{s)}$$

Tokamak Transport

- **Profile consistency (or profile resilience or stiffness)**

- The observation that profiles (of temperature, density, and pressure) often tend to adopt roughly the same shape (in tokamaks), regardless of the applied heating and fueling profiles.

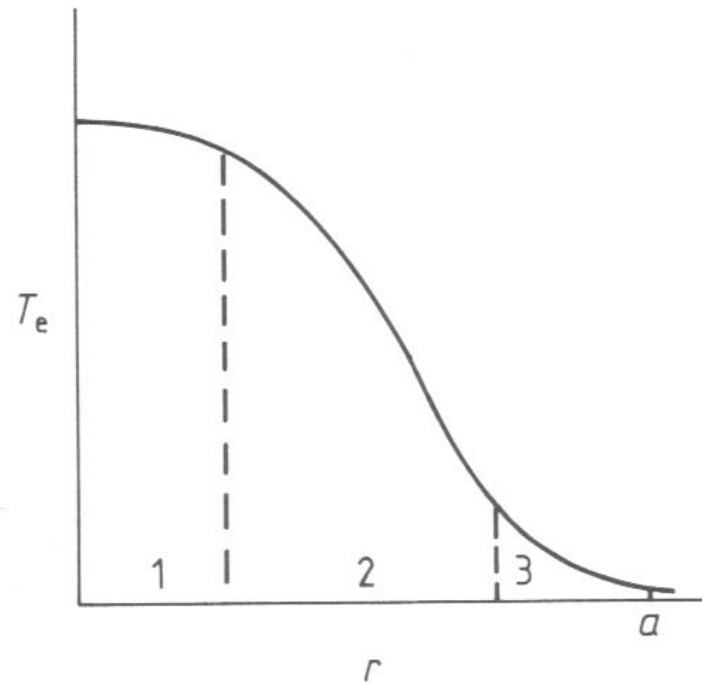
- B. Coppi, "*Nonclassical Transport and the "Principle of Profile Consistency"*",
Comments Plasma Phys. Cont. Fusion **5** 6 261-270 (1980)

- tendency of profiles to stay close to marginal stability

- Due to plasma self-organisation, i.e., the feedback mechanism regulating the profiles (by turbulence) is often dominant over the various source terms.

Tokamak Transport

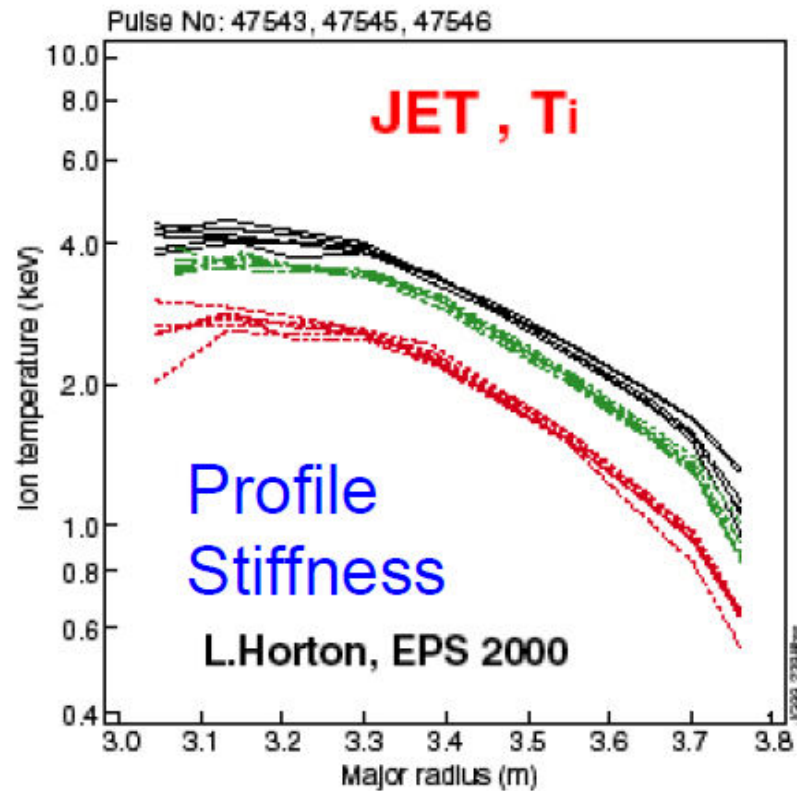
- Profile consistency (or profile resilience or stiffness)



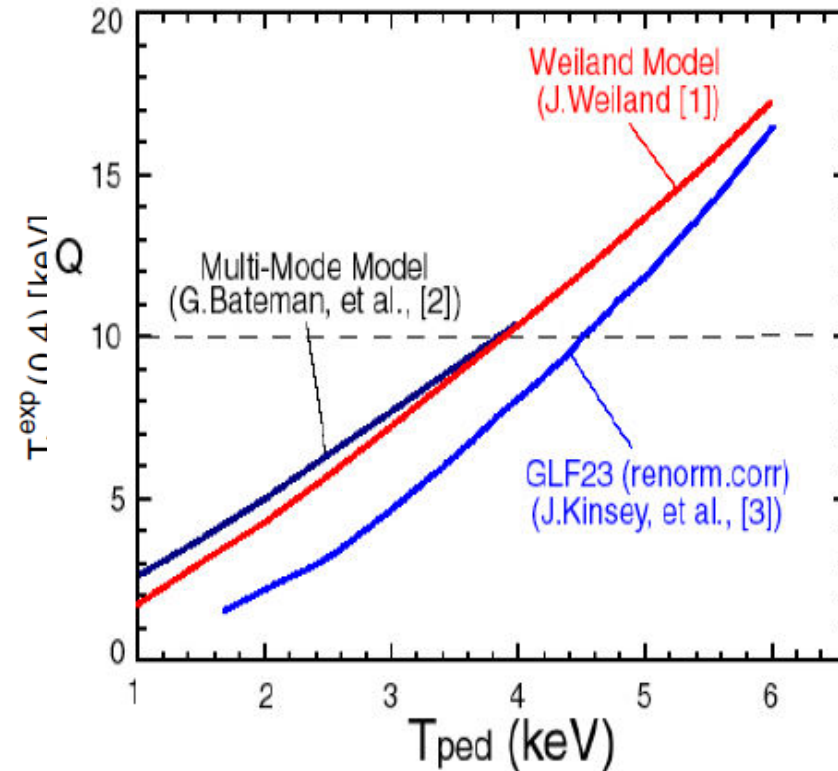
- Three zones in which transport processes play the dominant part
- 1: sawtooth oscillations - volume depending on the inversion radius which depending on q_a
- 2: heat transfer - responsible for magnetic confinement
- 3: atomic processes

Tokamak Transport

- Profile consistency (or profile resilience or stiffness)



ITER: $I=15\text{MA}$; $P_{\text{aux}}=40\text{MW}$; $n=0.85n_G$

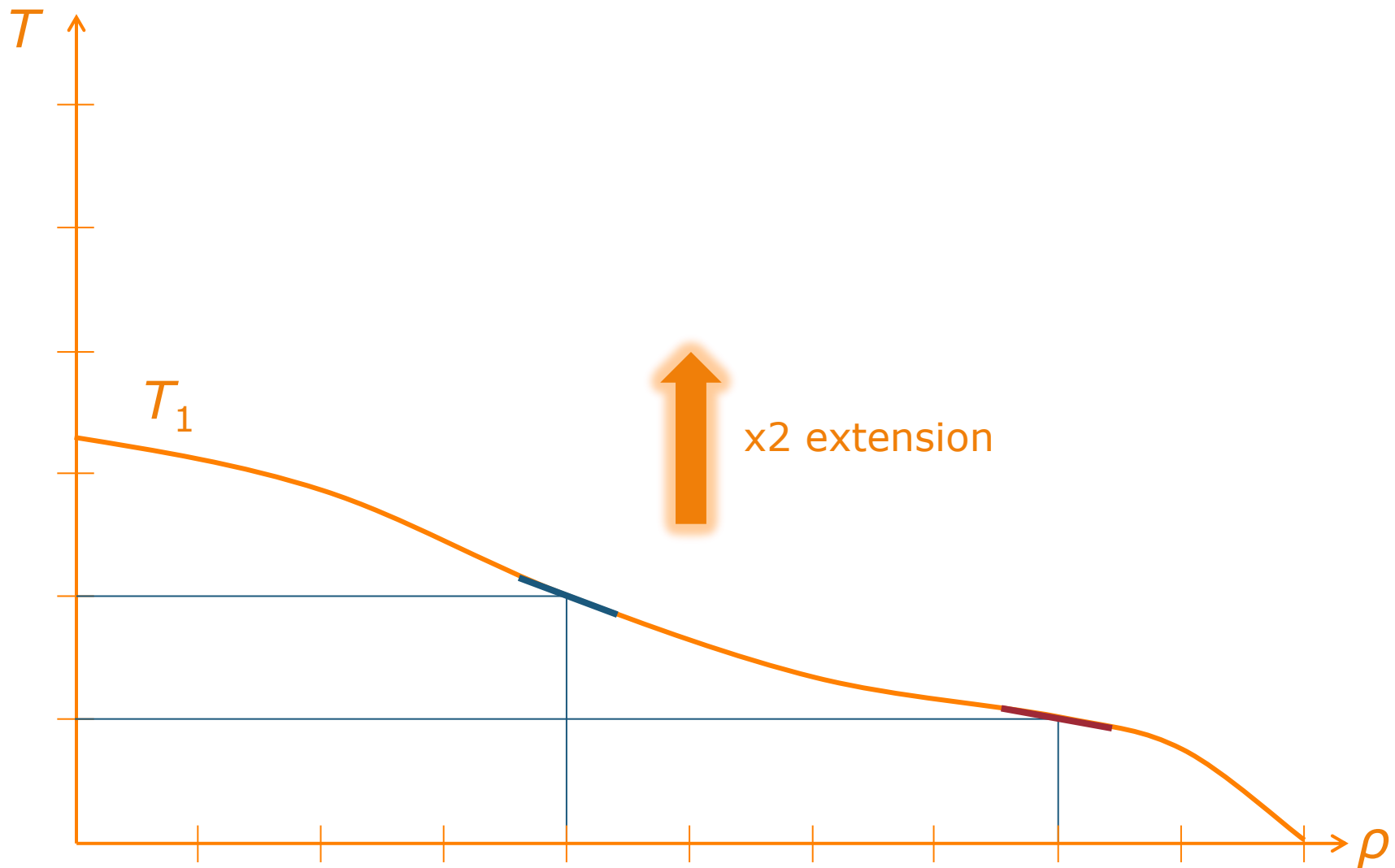


$$D^{\text{exp}} = D^{\text{NC}} + D^{\text{anomalous}} > D^{\text{NC}}$$

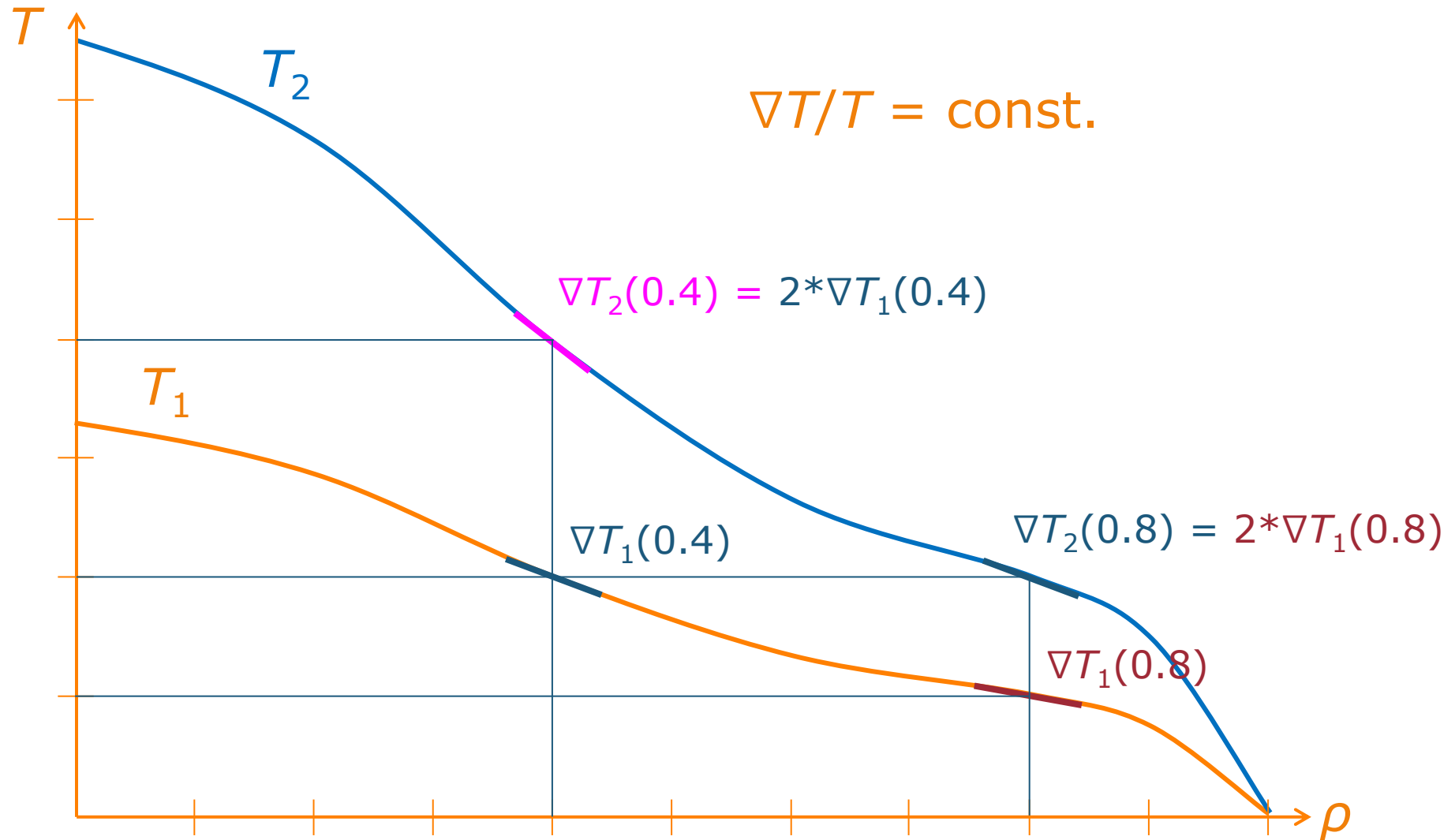
$$\chi^{\text{exp}} = \chi^{\text{NC}} + \chi^{\text{anomalous}} > \chi^{\text{NC}}$$



Tokamak Transport



Tokamak Transport



Tokamak Transport

- **Microinstabilities**

- often associated with non-Maxwellian velocity distributions: deviation from thermodynamic equilibrium (nonuniformity, anisotropy of distributions) → free energy source which can drive instabilities
- kinetic approach required: limited MHD approach

- **Two-stream or beam-plasma instability**

- Particle bunching → \mathbf{E} perturbation → bunching↑ → unstable

- **Drift (or Universal) instability**

- driven by ∇p (or ∇n) in magnetic field
- excited by drift waves with a phase velocity of v_{De} with a very short wavelength
- most unstable, dominant for anomalous transport

- **Trapped particle modes**

- Preferably when the perturbation frequency < bounce frequency
- drift instability enhanced by trapped particle effects
- Trapped Electron Mode (TEM), Trapped Ion Mode (TIM)

Tokamak Transport

- **Microinstabilities**

- Plasma waves and their associated instabilities

- Electron drift wave: 'Universal', trapped electron

- Sound wave: Ion temperature gradient

- Alfven wave: Micro-tearing

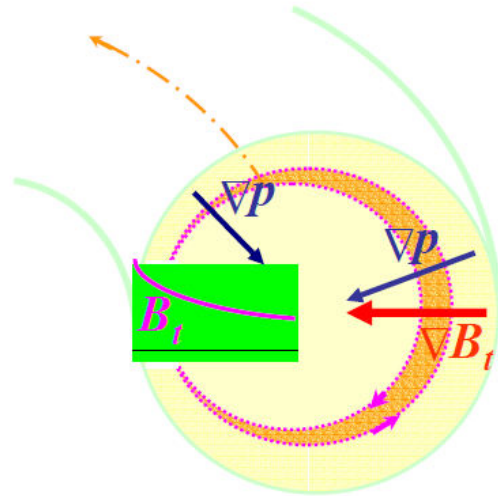
Tokamak Transport

- **Microinstabilities**

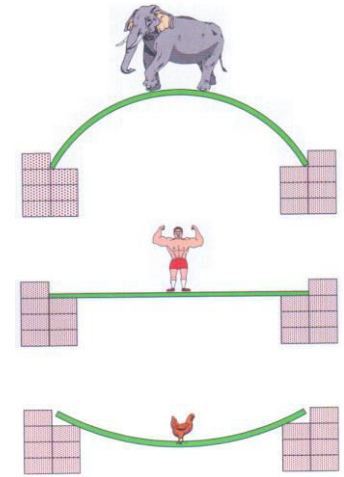
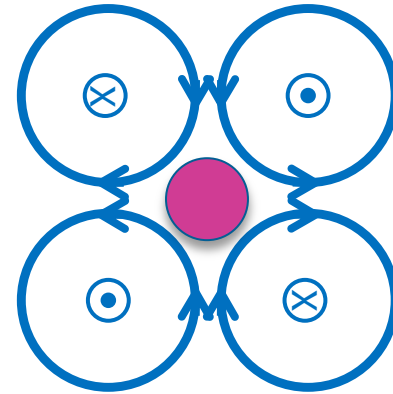
- Electrostatic instabilities: drift wave instabilities
perturbations of the magnetic field are ignored,
so that only the perturbed electric field matters.
Assumption appropriate if the plasma beta is lower than the
instability threshold for electromagnetic interchange modes
(called 'kinetic ballooning modes')
 - Passing particle instabilities
 - Trapped particle instabilities
 - Ex. Ion Temperature Gradient (ITG) modes,
Trapped Electron Modes (TEM)
- Electromagnetic instabilities: micro-tearing modes

Tokamak Transport

- Anomalous Transport



Unstable region: $\nabla B_t \cdot \nabla p > 0$



- Trapped particles are localised on the low field side, as this corresponds to the zone of minimum field along the field lines.
→ Trapped particles are expected to play a prominent role in the interchange process.

Tokamak Transport

- Transport dominated by turbulence

Ch. P. Ritz et al, PRL **62** 1844 (1989)
X. Garbet, C.R. Physique **7** 573 (2006)

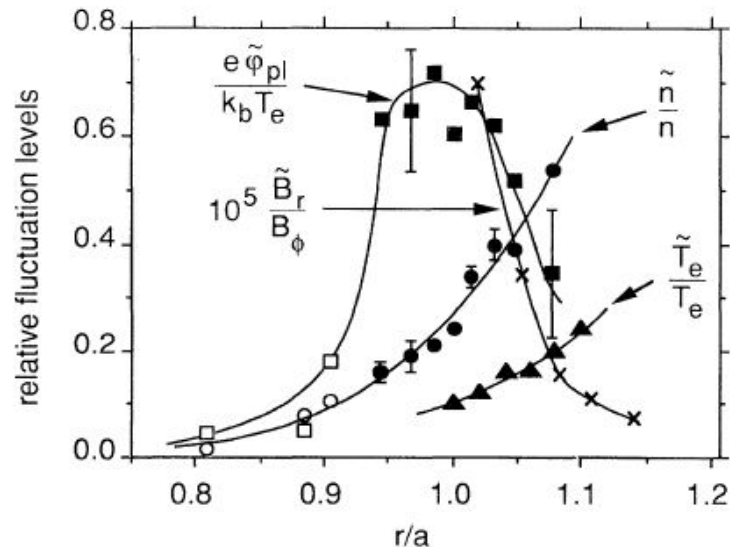


FIG. 1. Relative fluctuation levels of density \tilde{n}/n , plasma potential $e\tilde{\phi}_{pl}/k_B T_e$, electron temperature \tilde{T}_e/T_e , and magnetic field \tilde{B}_r/B_ϕ , as functions of radius. Filled symbols represent data from Langmuir probes, and open symbols from the HIBP.

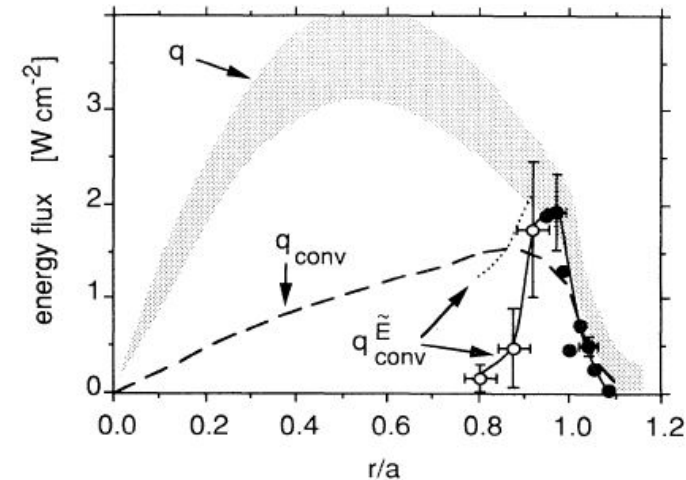


FIG. 2. Radial profiles of the total electron and ion energy flux $q = q_e + q_i$ from power balance (shaded area, defined by the standard deviation), the fluctuation-induced convected flux q_{conv}^E (filled circles from Langmuir probes, and open circles from HIBP; dotted line is upper bound in presence of η_i mode), and the total convected energy flux $q_{conv}(r)$ from a neutral-penetration code and H_α measurements.

- It was proved that in edge plasmas, turbulence particle and energy fluxes agree with the fluxes deduced from particle and heat balance (i.e., integral of the particle and heating sources). Since then, several studies have confirmed the close connection between turbulence and transport. In particular, a reduction of the fluctuation level is observed when a **transport barrier** is formed.

How to reduce plasma transport?

Tokamak Transport

• Suppression of Anomalous Transport: H-mode

- 1982 IAEA FEC, F. Wagner et al. (ASDEX, Germany)
- Transition to H-mode: state with reduced turbulence at the plasma edge
- Formation of an edge transport barrier: steep pressure gradient at the edge

Regime of Improved Confinement and High Beta in Neutral-Beam-Heated Divertor Discharges of the ASDEX Tokamak

F. Wagner, G. Becker, K. Behringer, D. Campbell, A. Eberhagen, W. Engelhardt, G. Fussmann, O. Gehre, J. Gernhardt, G. v. Gierke, G. Haas, M. Huang,^(a) F. Karger, M. Keilhacker, O. Klüber, M. Kornherr, K. Lackner, G. Lisitano, G. G. Lister, H. M. Mayer, D. Meisel, E. R. Müller, H. Murmann, H. Niedermeyer, W. Poschenrieder, H. Rapp, H. Röhr, F. Schneider, G. Siller, E. Speth, A. Stäbler, K. H. Steuer, G. Venus, O. Vollmer, and Z. Yü^(a)

Max-Planck-Institut für Plasmaphysik, EURATOM-Association, D-8046 Garching, München, Germany
(Received 6 August 1982; revised manuscript received 1 October 1982)

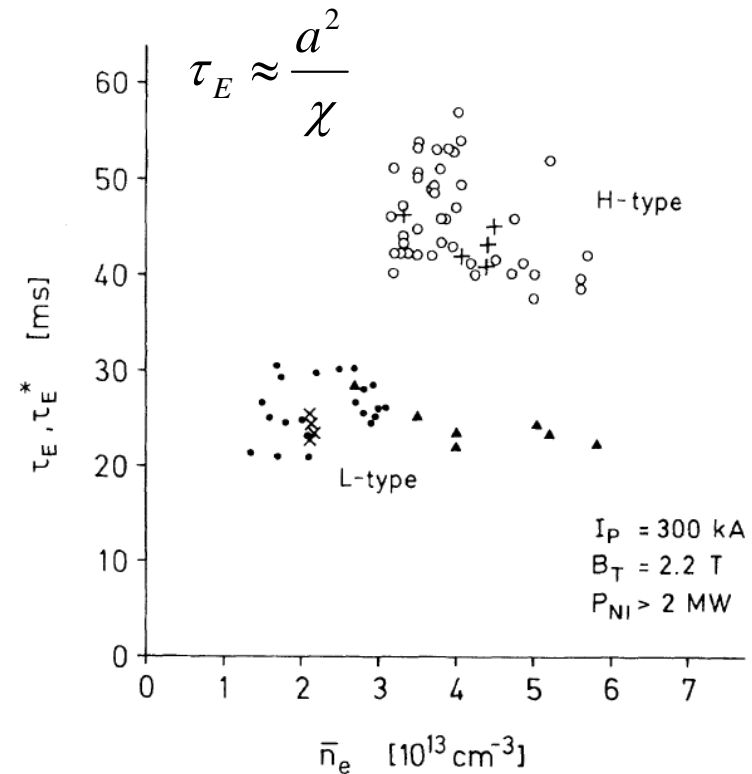
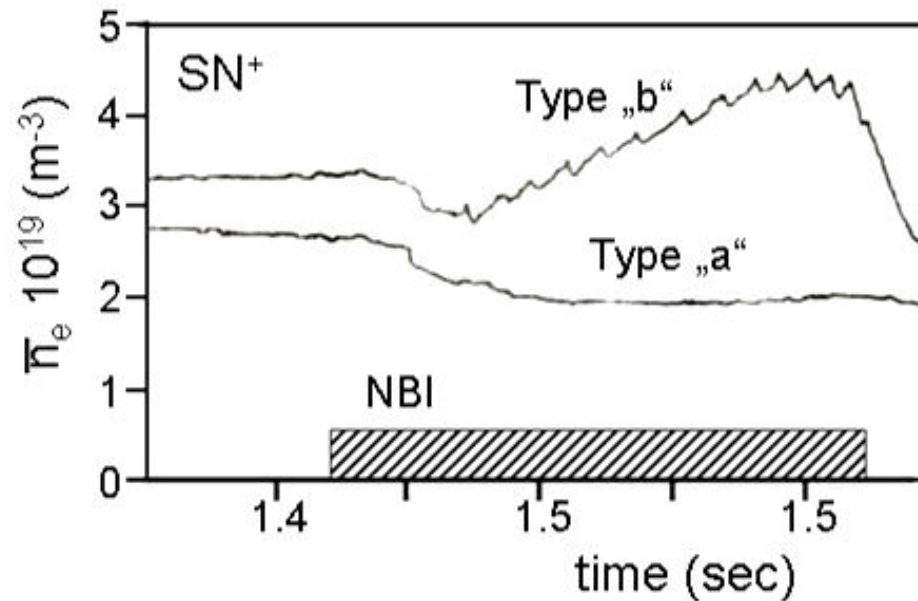
A new operational regime has been observed in neutral-injection-heated ASDEX divertor discharges. This regime is characterized by high β_p values comparable to the aspect ratio A ($\beta_p \leq 0.65A$) and by confinement times close to those of Ohmic discharges. The high- β_p regime develops at an injection power ≥ 1.9 MW, a mean density $\bar{n}_e \geq 3 \times 10^{13}$ cm⁻³, and a $q(a)$ value ≥ 2.6 . Beyond these limits or in discharges with material limiter, low β_p values and reduced particle and energy confinement times are obtained compared to the Ohmic heating phase.

PACS numbers: 52.55.Gb, 52.50.Gj

Tokamak Transport

• Suppression of Anomalous Transport: H-mode

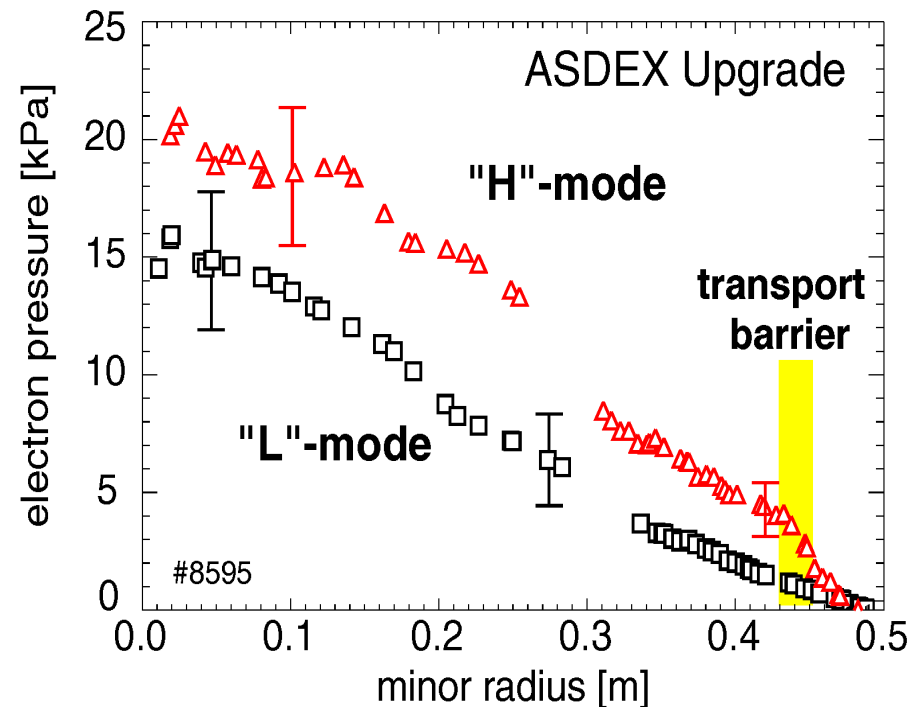
- 1982 IAEA FEC, F. Wagner et al. (ASDEX, Germany)
- Transition to H-mode: state with reduced turbulence at the plasma edge
- Formation of an edge transport barrier: steep pressure gradient at the edge



Tokamak Transport

• Suppression of Anomalous Transport: H-mode

- 1982 IAEA FEC, F. Wagner et al. (ASDEX, Germany)
- Transition to H-mode: state with reduced turbulence at the plasma edge
- Formation of an edge transport barrier: steep pressure gradient at the edge

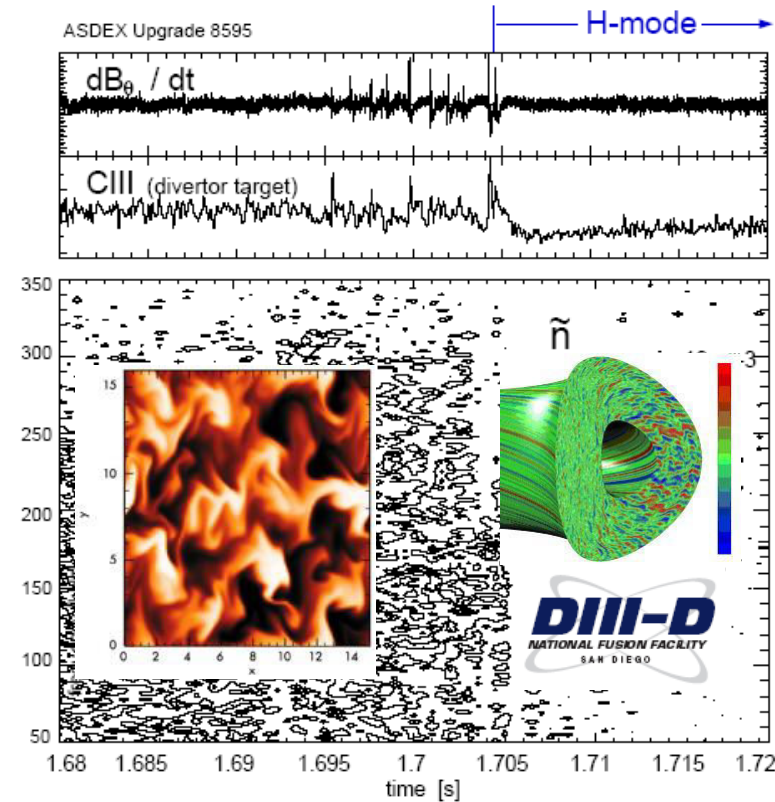
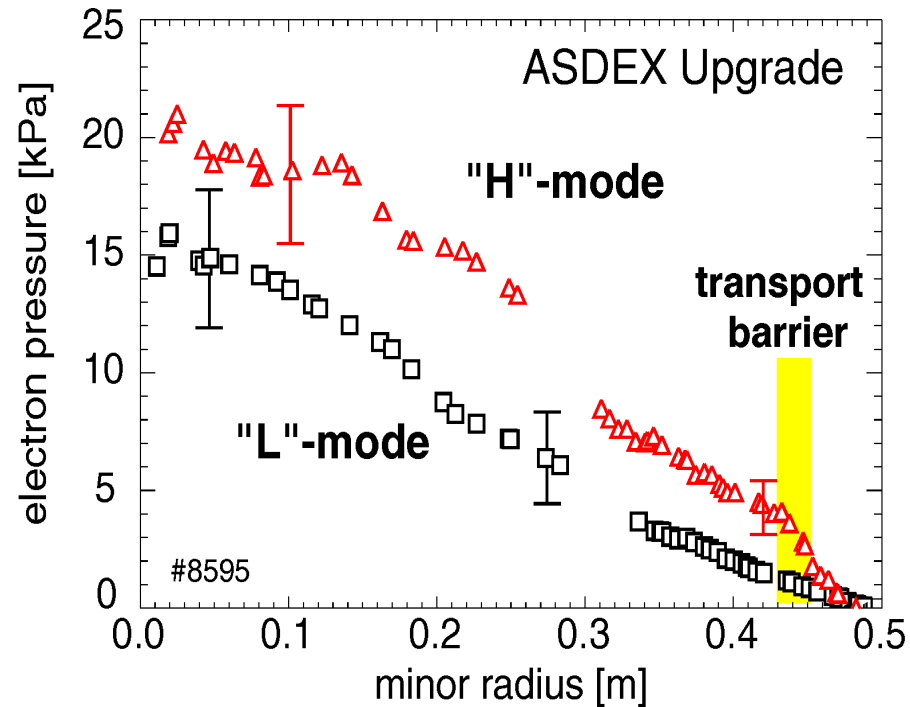


Hoover dam

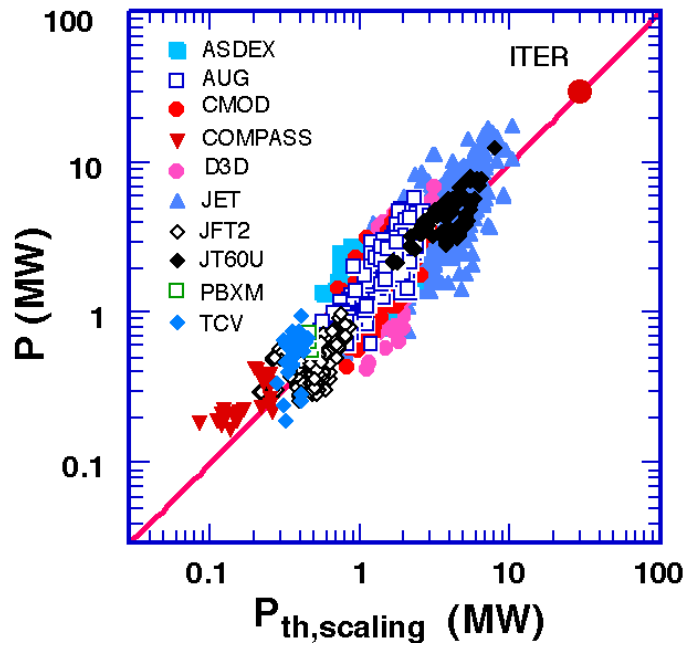
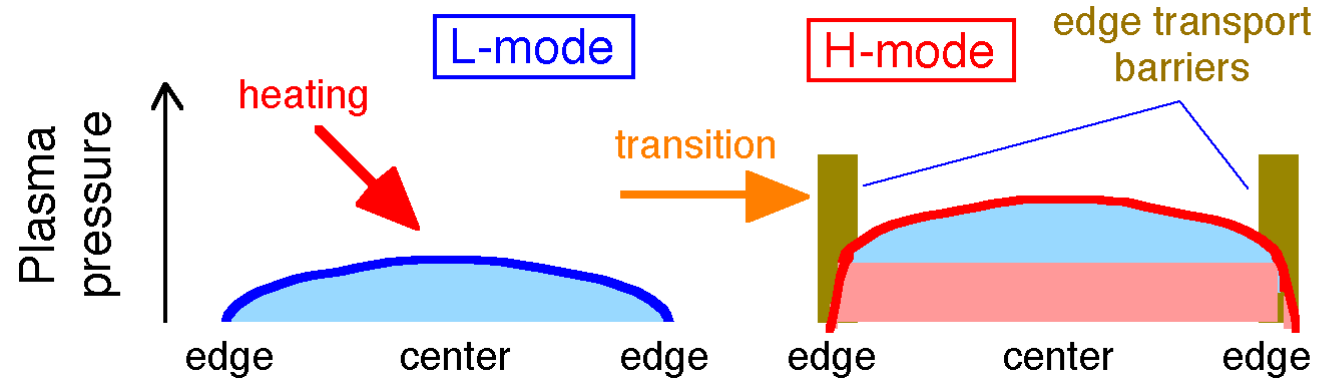
Tokamak Transport

• Suppression of Anomalous Transport: H-mode

- 1982 IAEA FEC, F. Wagner et al. (ASDEX, Germany)
- Transition to H-mode: state with reduced turbulence at the plasma edge
- Formation of an edge transport barrier: steep pressure gradient at the edge



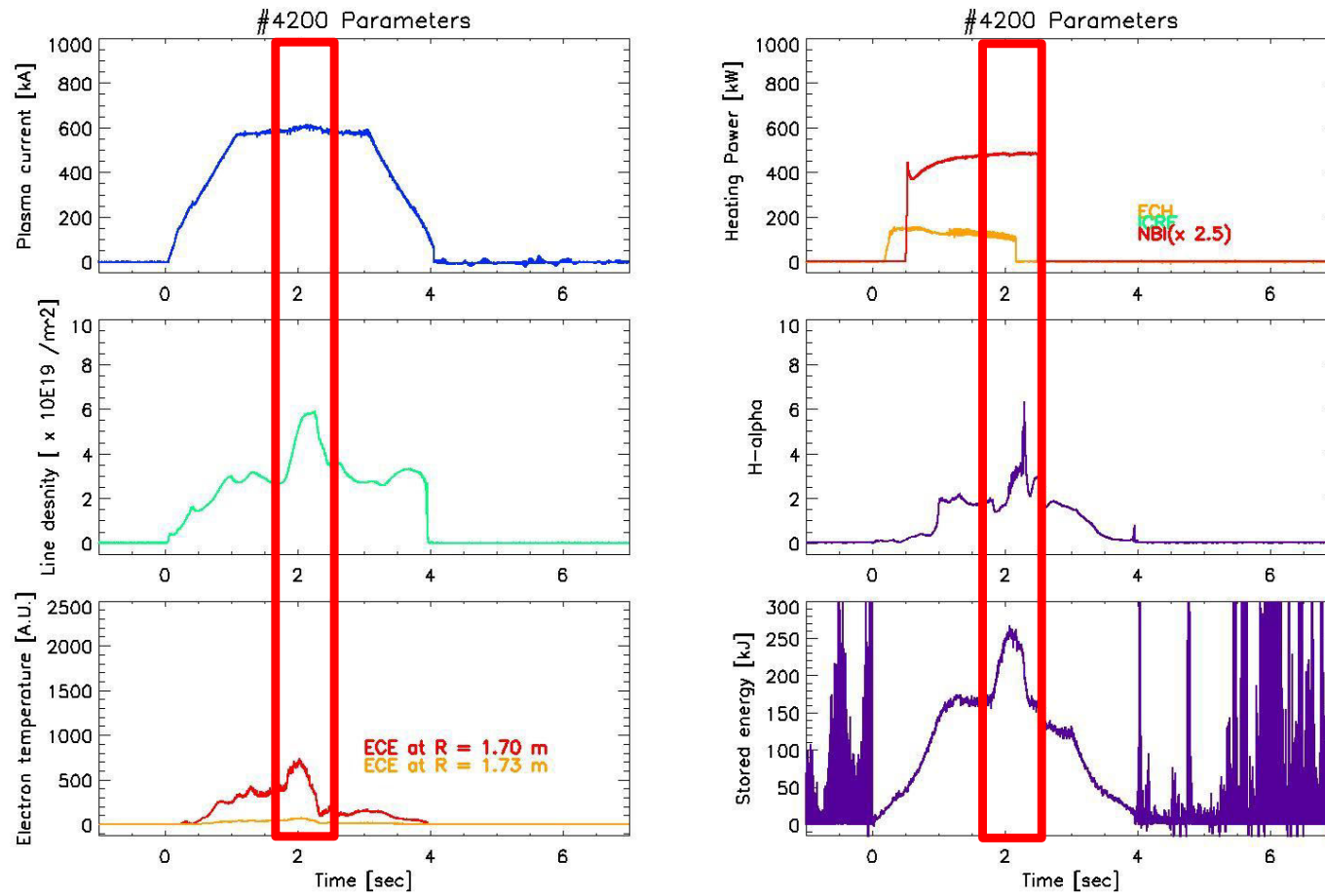
L-H transition threshold power



$$P_{th} = 2.84 M^{-1} B_t^{0.82} n_{20}^{0.58} R^{1.0} a^{0.81}$$

Tokamak Transport

- First H-mode Transition in KSTAR (November 8, 2010)



- $B_0 = 2.0 \text{ T}$, Heating = 1.5 MW (NBI : 1.3 MW, ECH : 0.2 MW)
After Boronisation on November 7, 2010

Tokamak Transport

- First H-mode Transition in KSTAR (November 8, 2010)

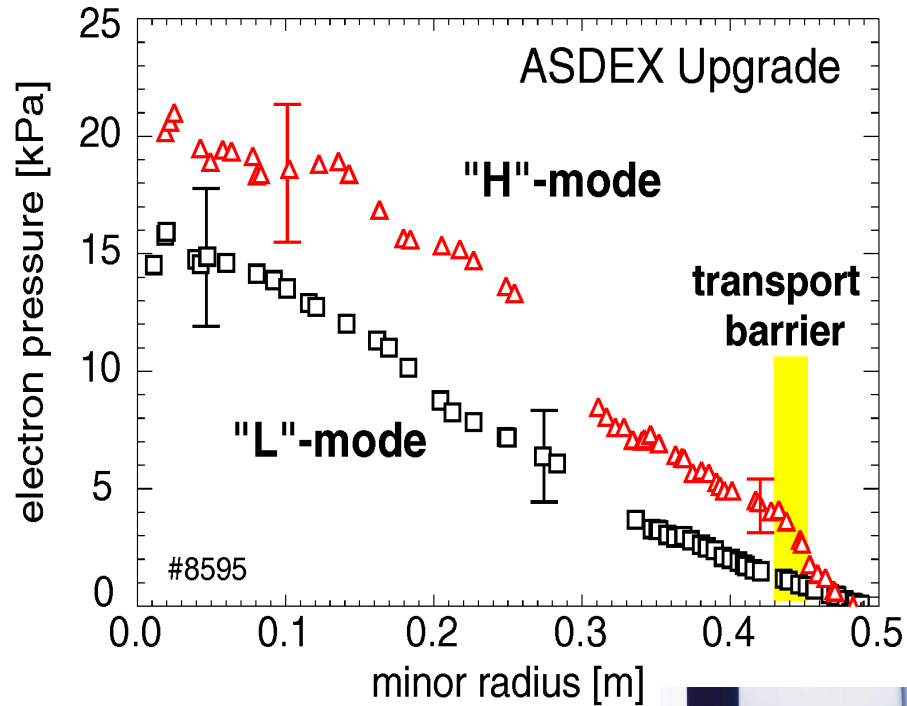


Tokamak Transport

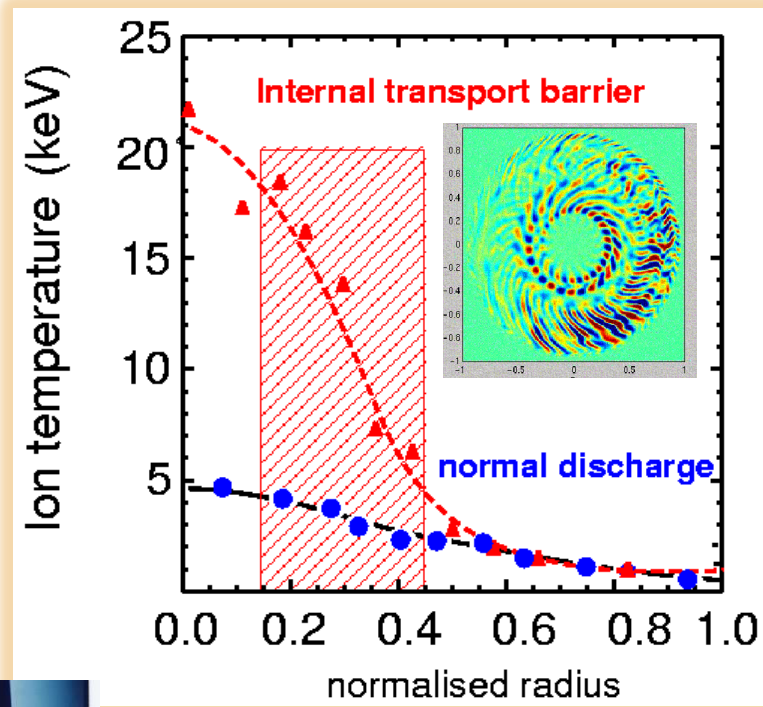
- **Suppression of Anomalous Transport: ITBs**



H-mode

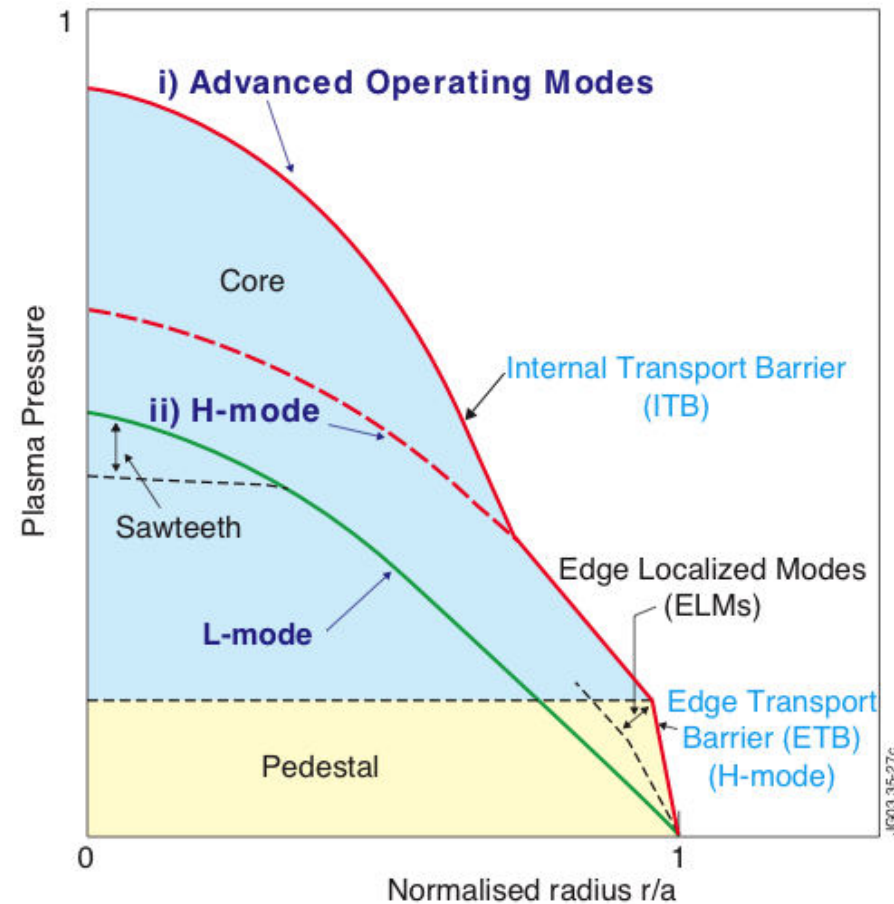


Reversed shear mode



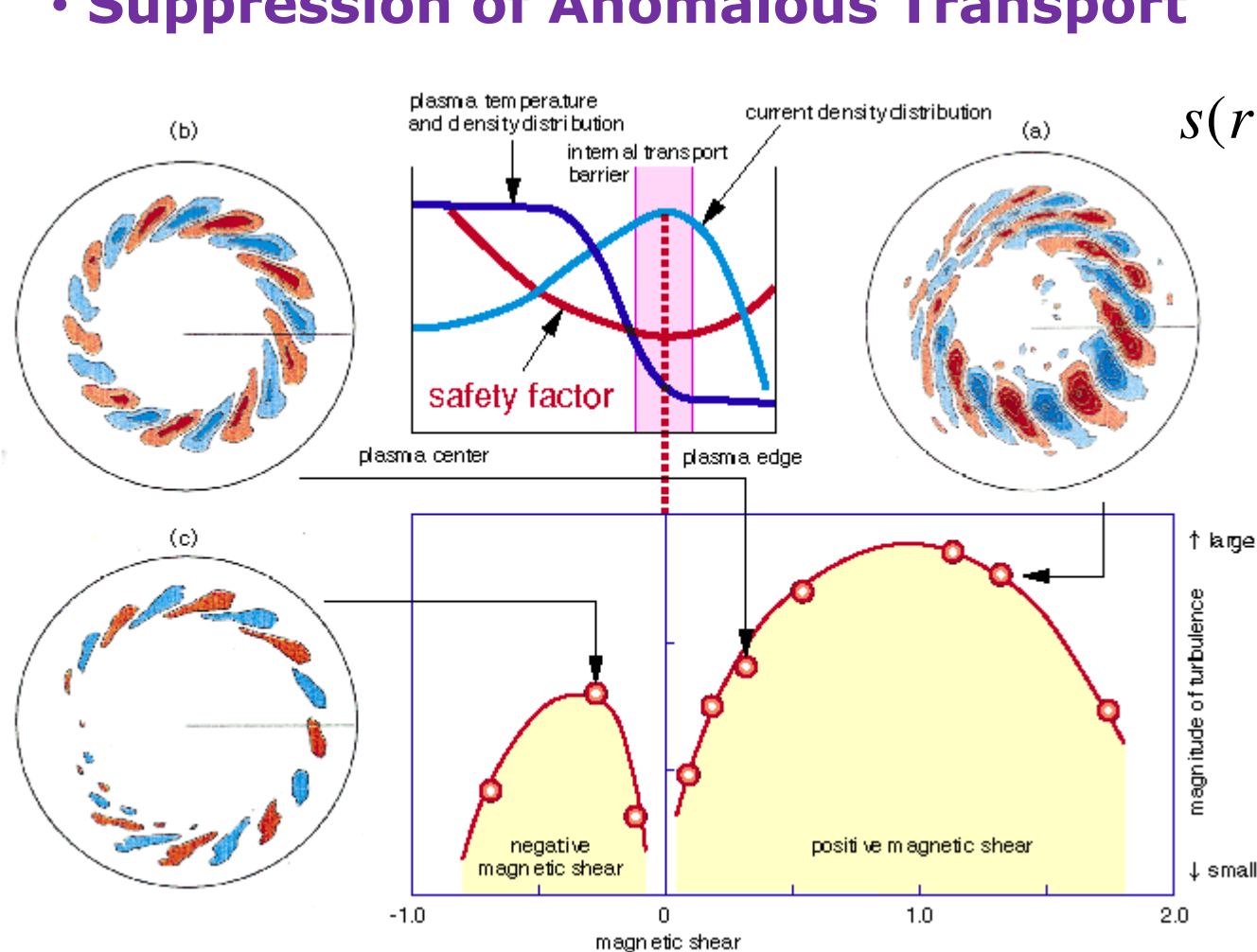
Tokamak Transport

- **Suppression of Anomalous Transport**

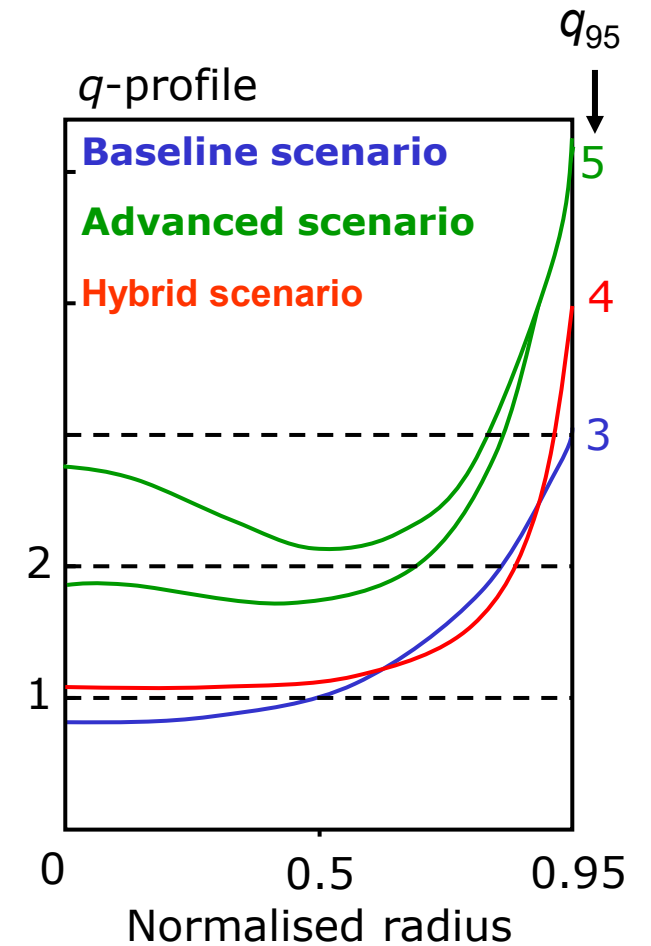


Tokamak Transport

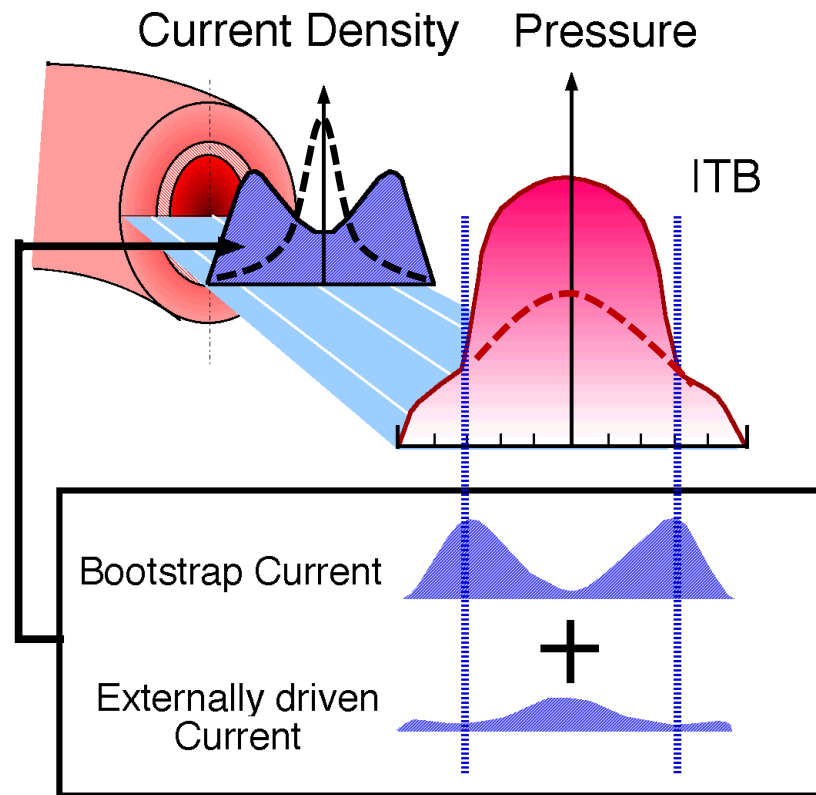
• Suppression of Anomalous Transport



$$s(r) \equiv \frac{r}{q} \frac{dq}{dr}$$



Improved confinement suitable for the steady-state operation



$$J_{BS} \propto \nabla p$$

Non-monotonic current profile



Turbulence suppression



High pressure gradients



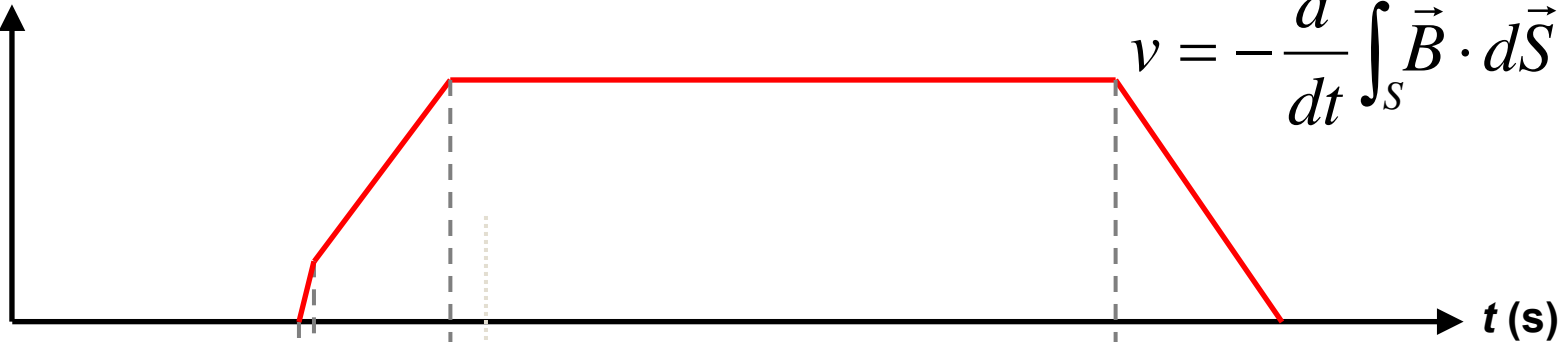
Large bootstrap current



Non-inductive current drive

Pulsed Operation

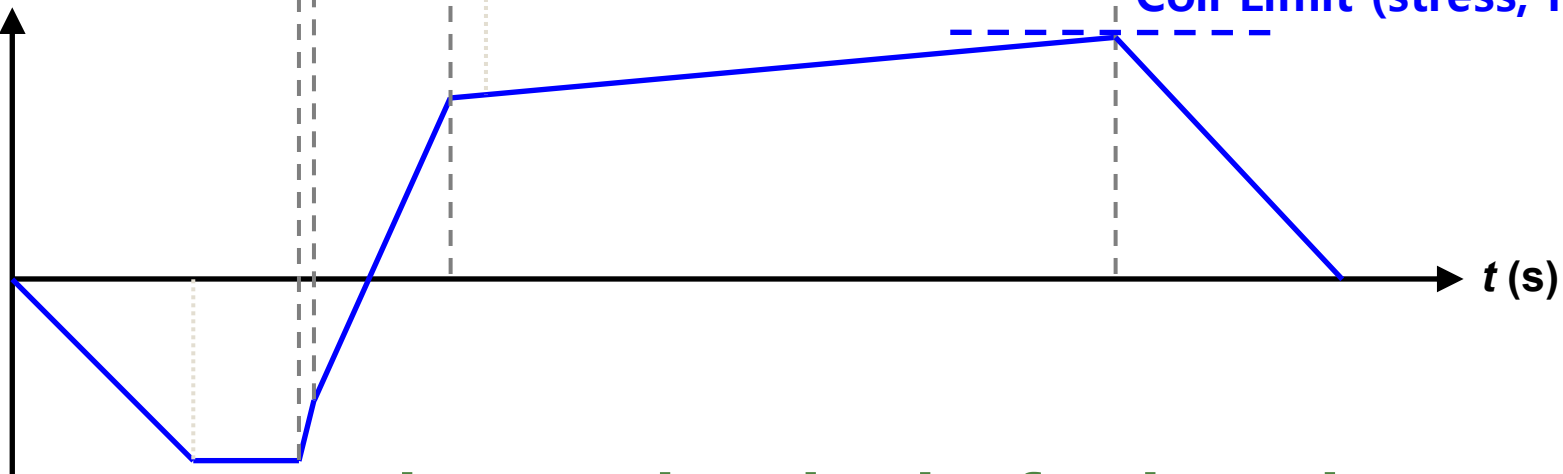
Plasma Current
(MA)



Faraday's law

$$v = -\frac{d}{dt} \int_s \vec{B} \cdot d\vec{S}$$

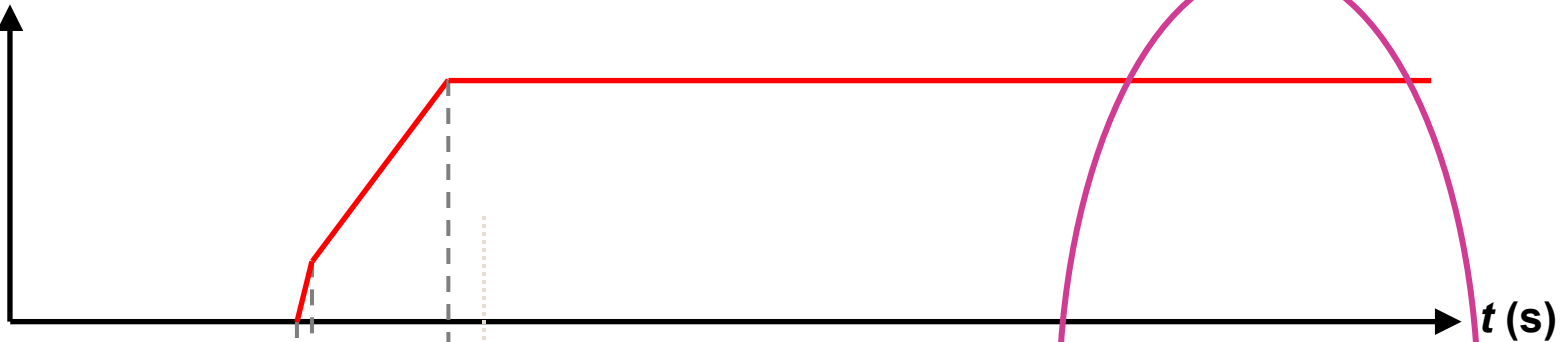
CS Coil Current
(kA)



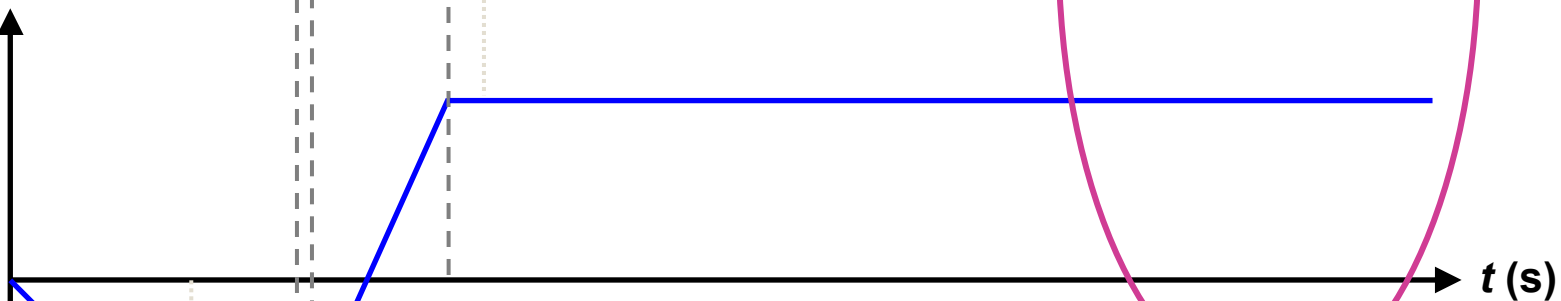
Inherent drawback of Tokamak!

Steady-State Operation

Plasma Current
(MA)



CS Coil Current
(kA)

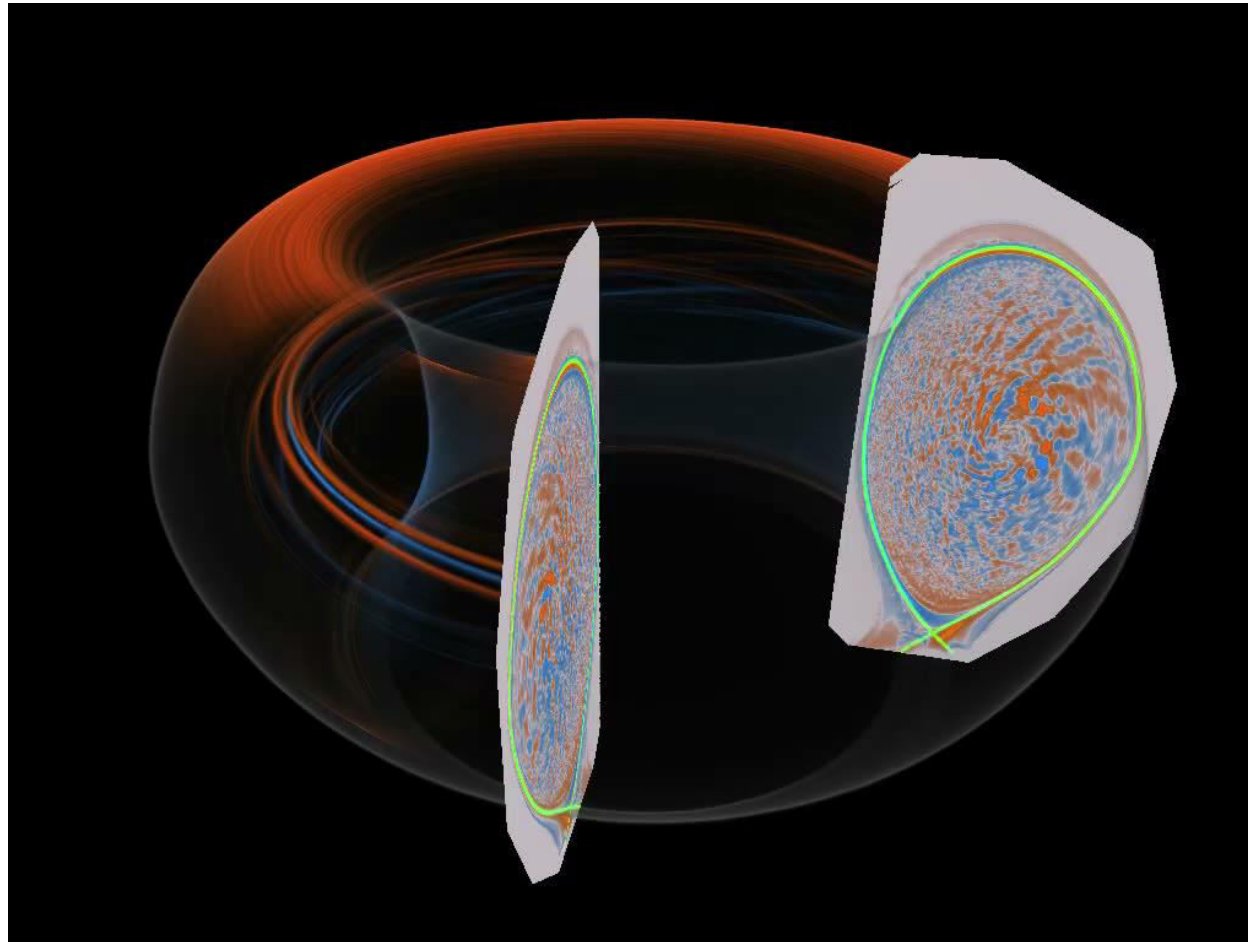


$$d/dt \sim 0$$

**Steady-state operation
by self-generated and externally driven current**

Turbulence Simulations

- XGC1 simulation



Turbulence Simulations

**Gyrokinetic Simulations
of Plasma Microinstabilities**

simulation by

Zhihong Lin et al.

Science 281, 1835 (1998)

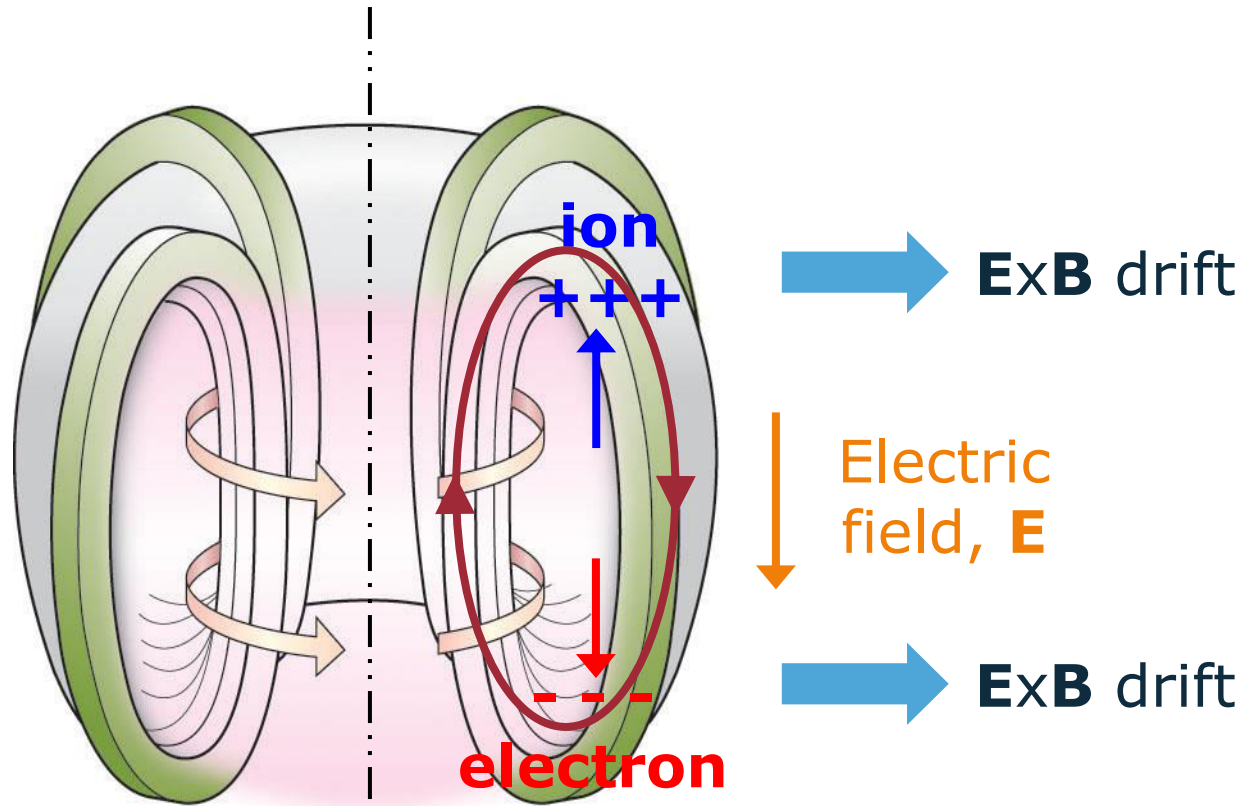
Introduction to Nuclear Fusion

Prof. Dr. Yong-Su Na

What is a stellarator?

M. Otthe, "Stellarator: Experiments", IPP Summer School (2008)

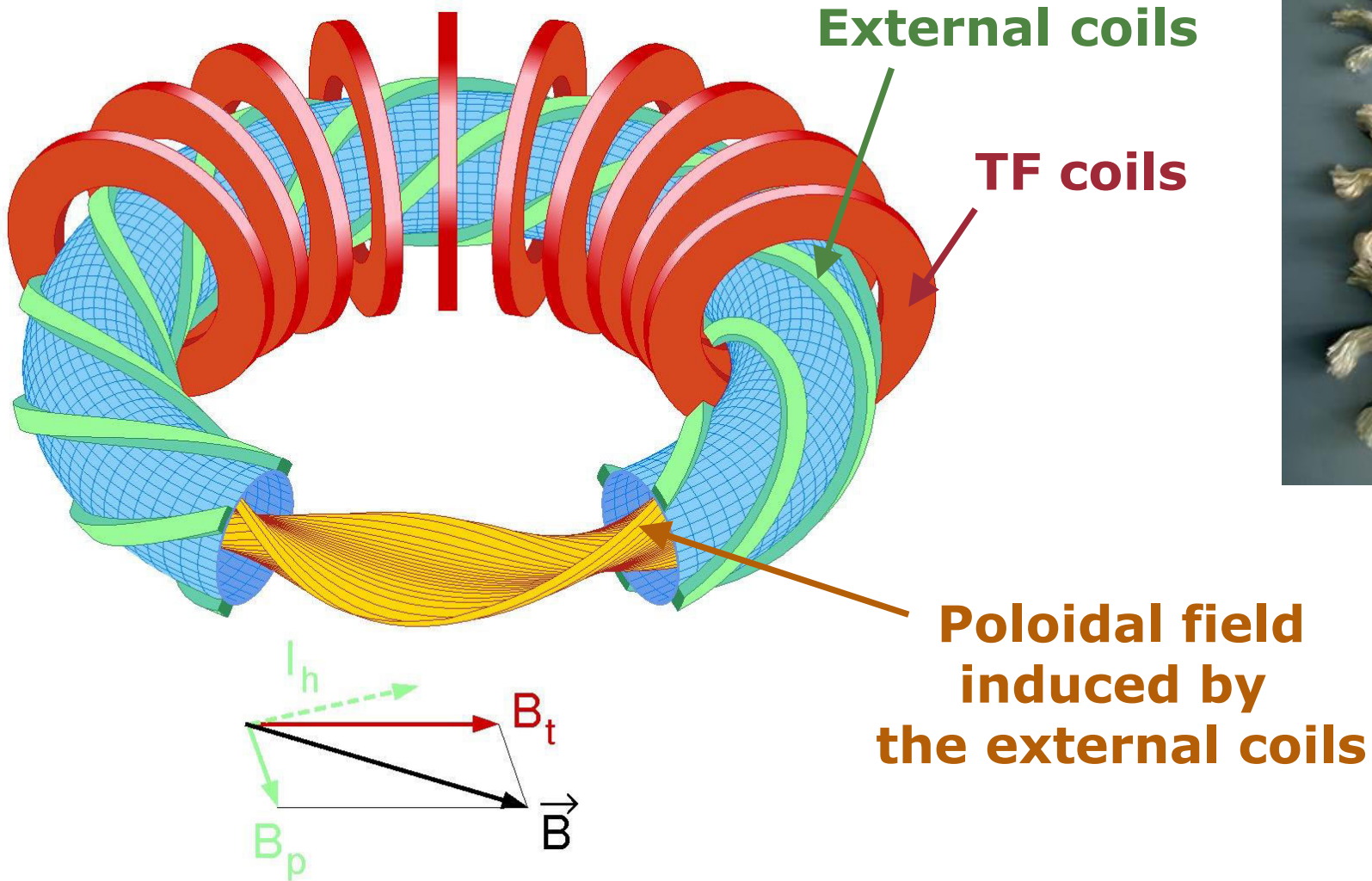
Closed Magnetic System



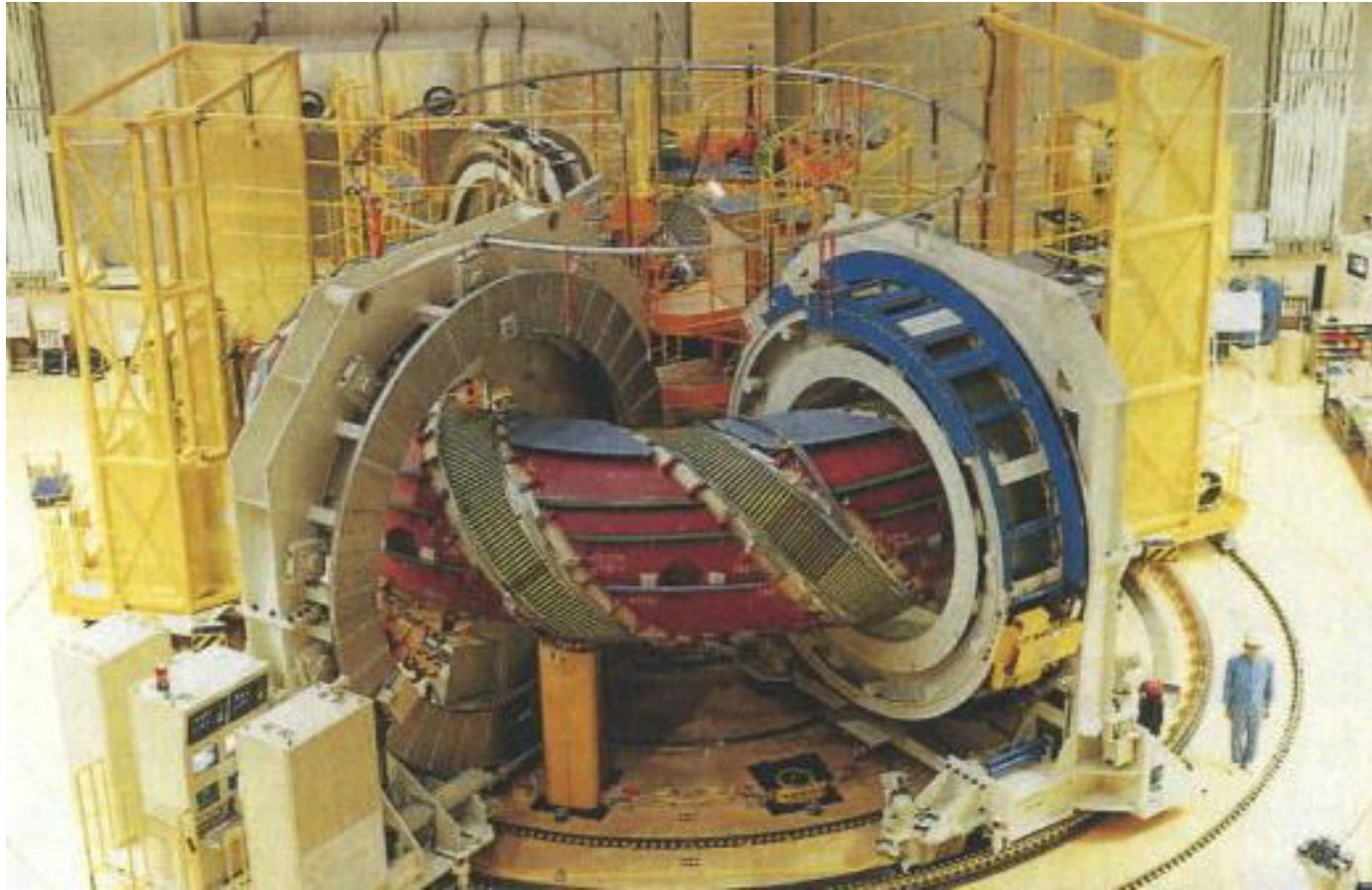
Poloidal magnetic field required

External coils → Stellarator

Stellarator



Stellarator



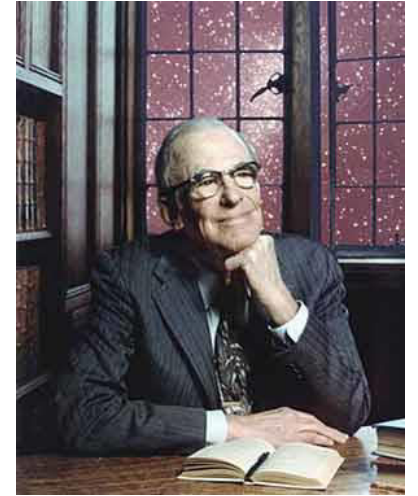
LHD (Large Helical Device) under construction

Stellarator

THE PHYSICS OF FLUIDS

VOLUME 1, NUMBER 4

JULY-AUGUST, 1958



The Stellarator Concept*

LYMAN SPITZER, JR.

Project Matterhorn, Princeton University, Princeton, New Jersey

(Received May 27, 1958)

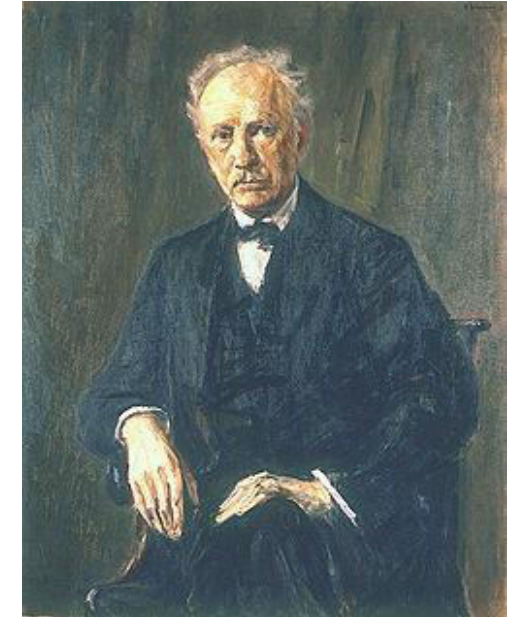
The basic concepts of the controlled thermonuclear program at Project Matterhorn, Princeton University are discussed. In particular, the theory of confinement of a fully ionized gas in the magnetic configuration of the stellarator is given, the theories of heating are outlined, and the bearing of observational results on these theories is described.

Stellarator

Invented by Lyman Spitzer, Jr. in Princeton in 1951



Garmisch-Partenkirchen,
Germany



Richard Georg Strauss
(1864 – 1949)



Stellarator

Invented by Lyman Spitzer, Jr. in Princeton in 1951

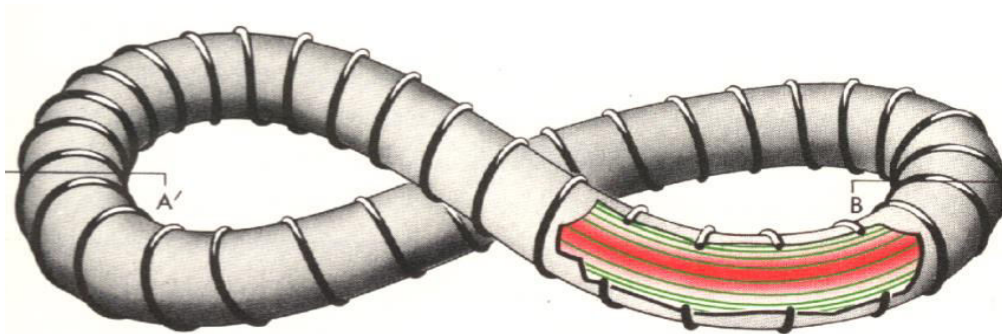
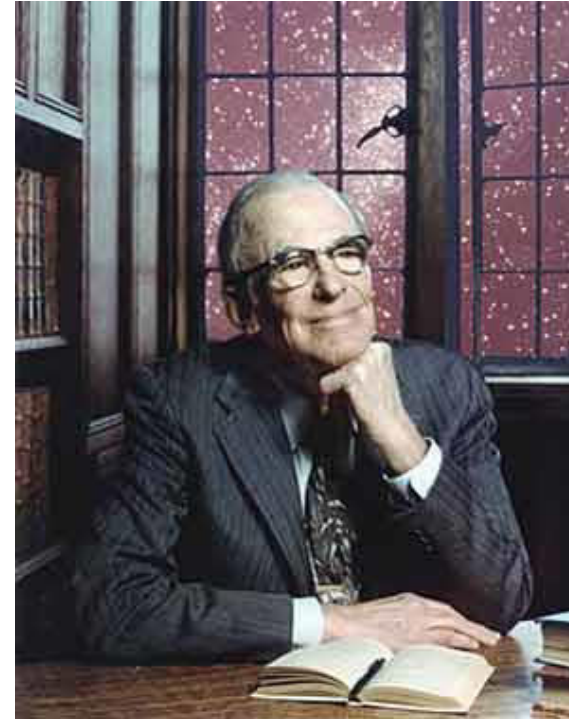
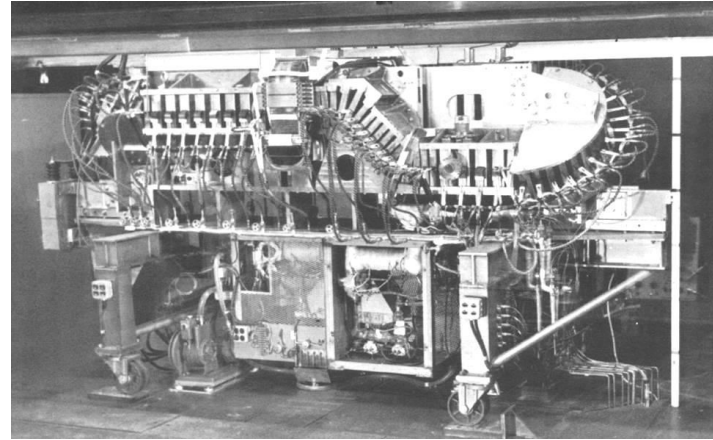
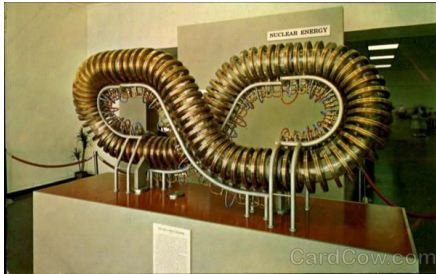
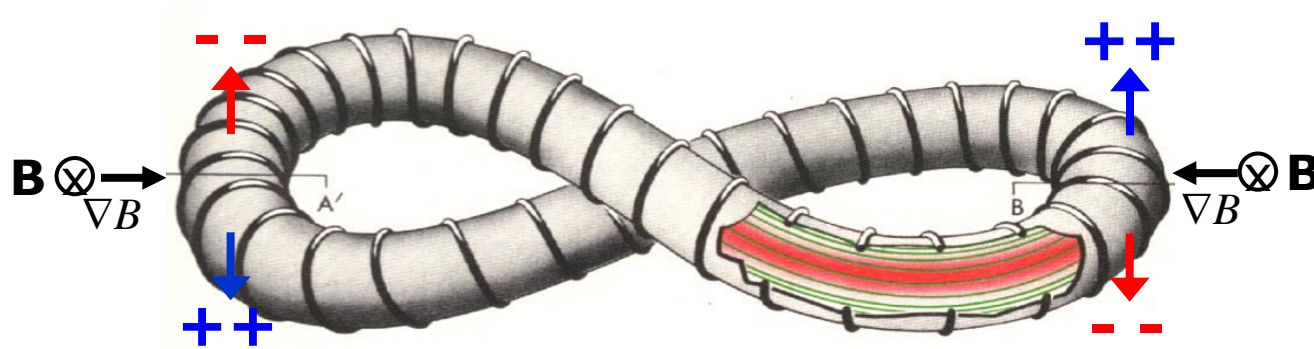
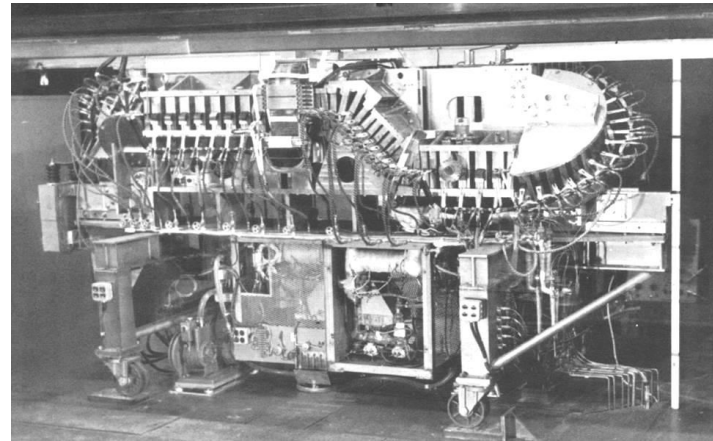
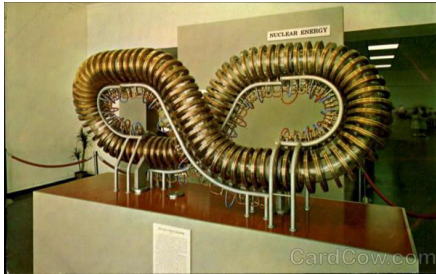


Figure-8 stellarator: Proof of principle experiment (helicity achieved by twisting the torus and hence the magnetic field)



Stellarator

Invented by Lyman Spitzer, Jr. in Princeton in 1951



$$\mathbf{v}_{D,R} = \frac{mv_{\parallel}^2}{qB_0^2} \frac{\mathbf{R}_0 \times \mathbf{B}_0}{R^2}$$

$$\begin{aligned} \mathbf{v}_{D,\nabla B} &= \pm \frac{1}{2} v_{\perp} r_L \frac{\mathbf{B} \times \nabla B}{B^2} \\ &= \frac{mv_{\perp}^2}{2qB} \frac{\mathbf{B} \times \nabla B}{B^2} \end{aligned}$$

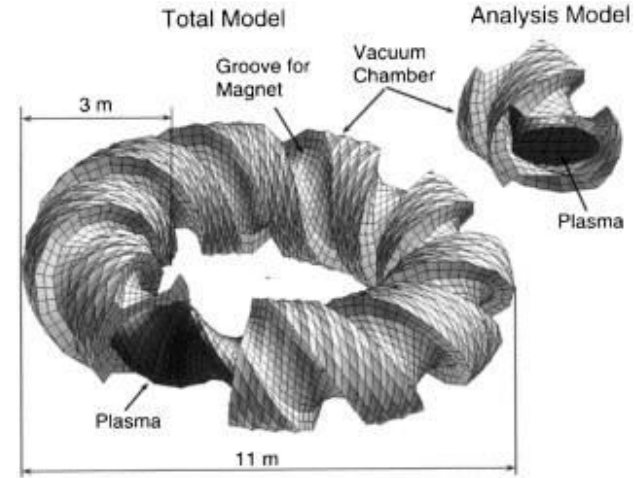
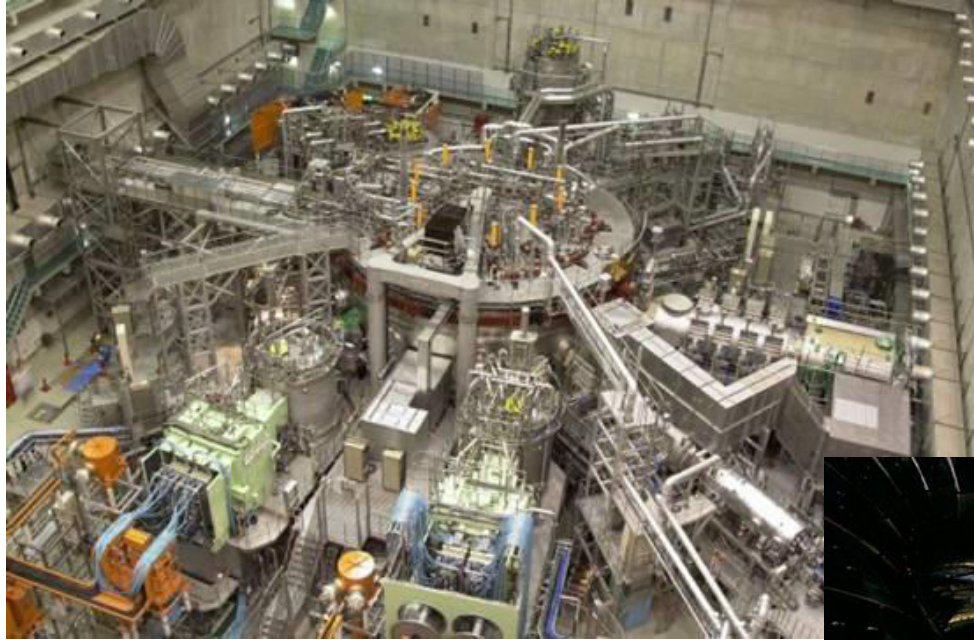
Figure-8 stellarator: Proof of principle experiment (helicity achieved by twisting the torus and hence the magnetic field)



WIKIPEDIA

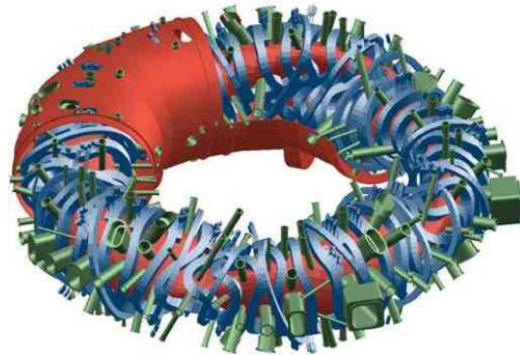
Stellarator

Large Helical Device (LHD), Japan

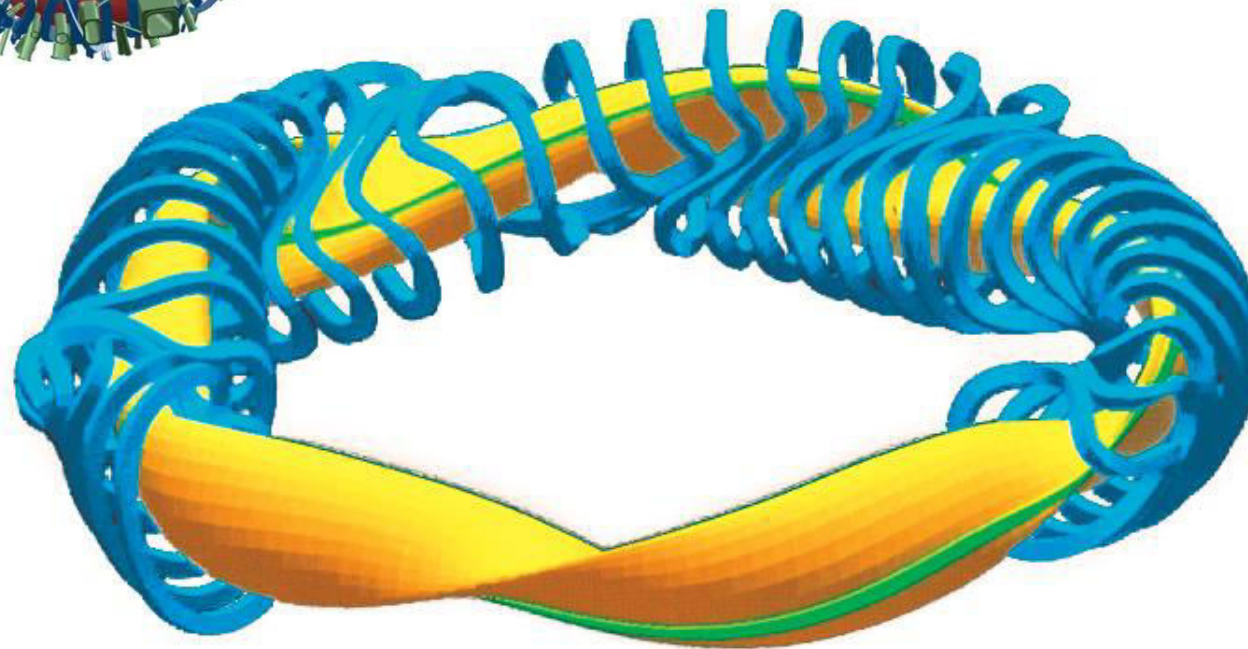


3D configuration!

Stellarator



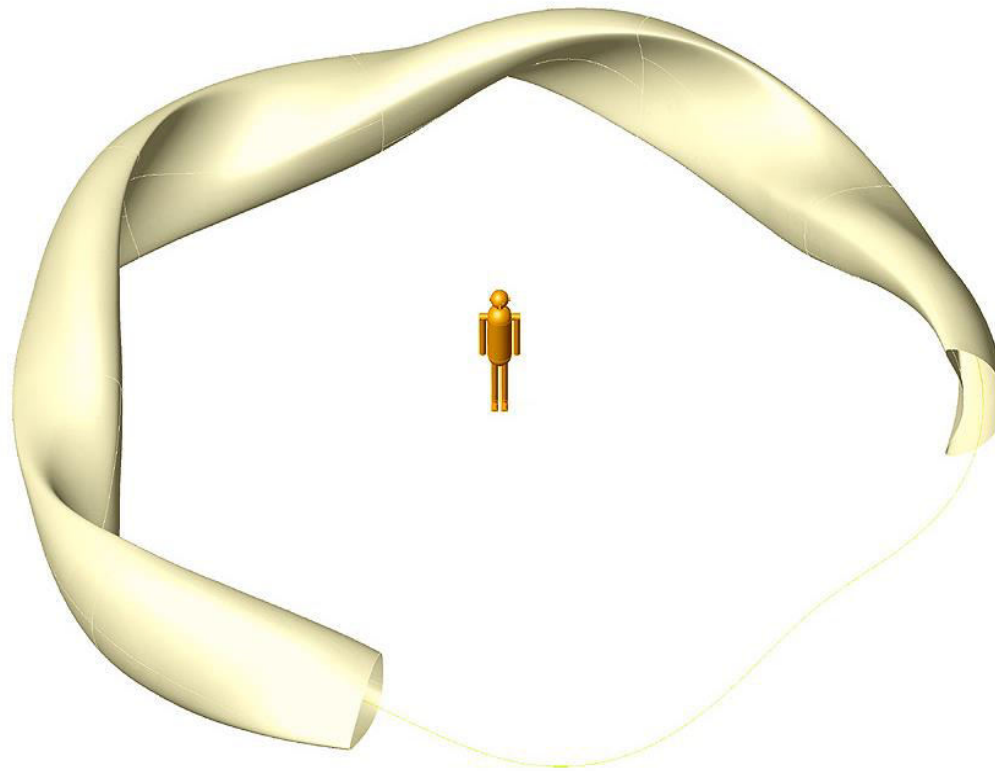
Wendelstein 7-X, Germany



3D configuration!

Stellarator

Plasma



Plasma Parameter

R : 5.5 m

$\langle a \rangle$: 0.53 m

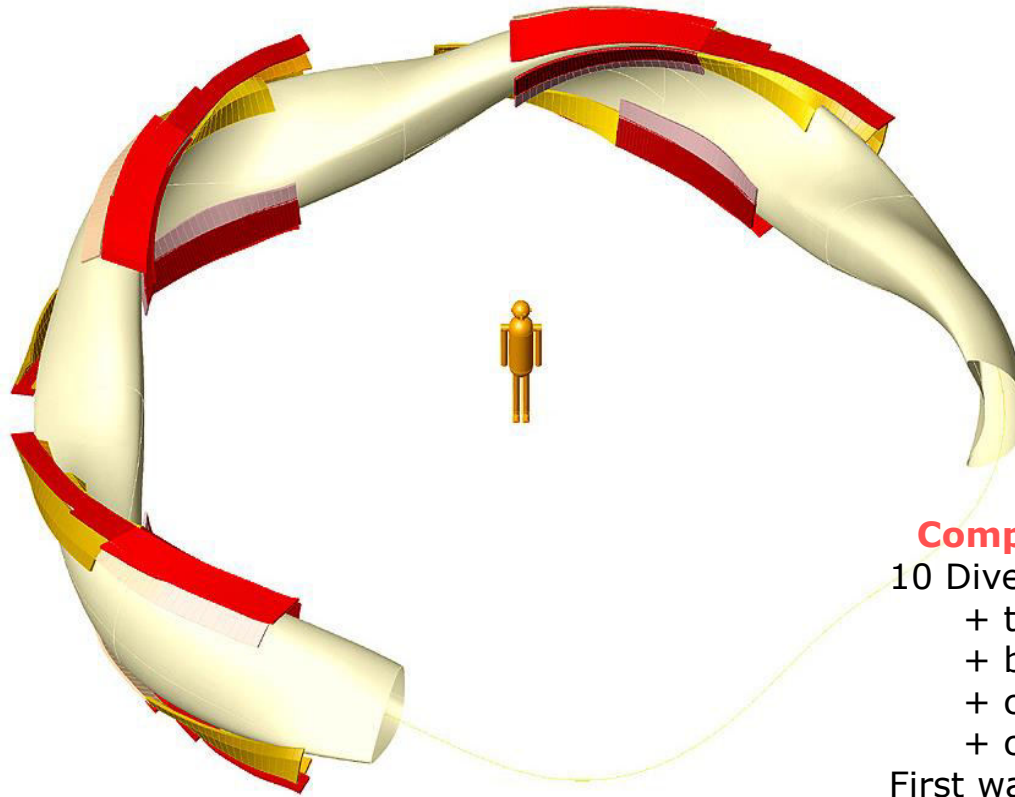
$n_e(0)_{\max}$: $3 \times 10^{20} \text{ m}^{-3}$

$T_e(0)_{\max}$: 5 keV

$\langle \beta \rangle$: < 5 %

Stellarator

Divertor



Components inside plasma vessel

10 Divertor units

+ target elements (10 MW/m²)

+ baffle elements (0.5 MW/m²)

+ control coils

+ cryo pumps

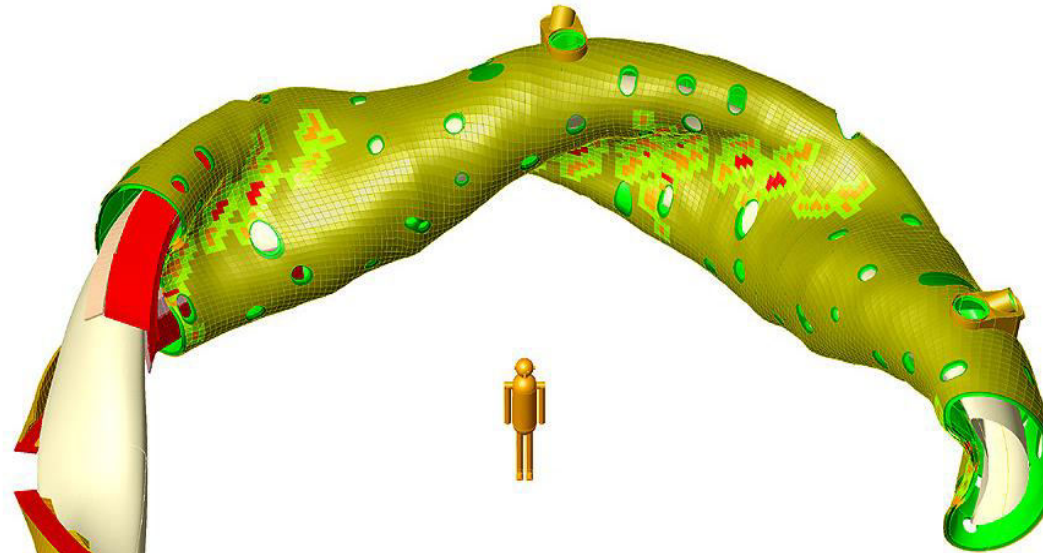
First wall with B₄C coating (0.2 MW/m²)

Diagnostics

- Design for steady state operation -

Stellarator

Plasma Vessel

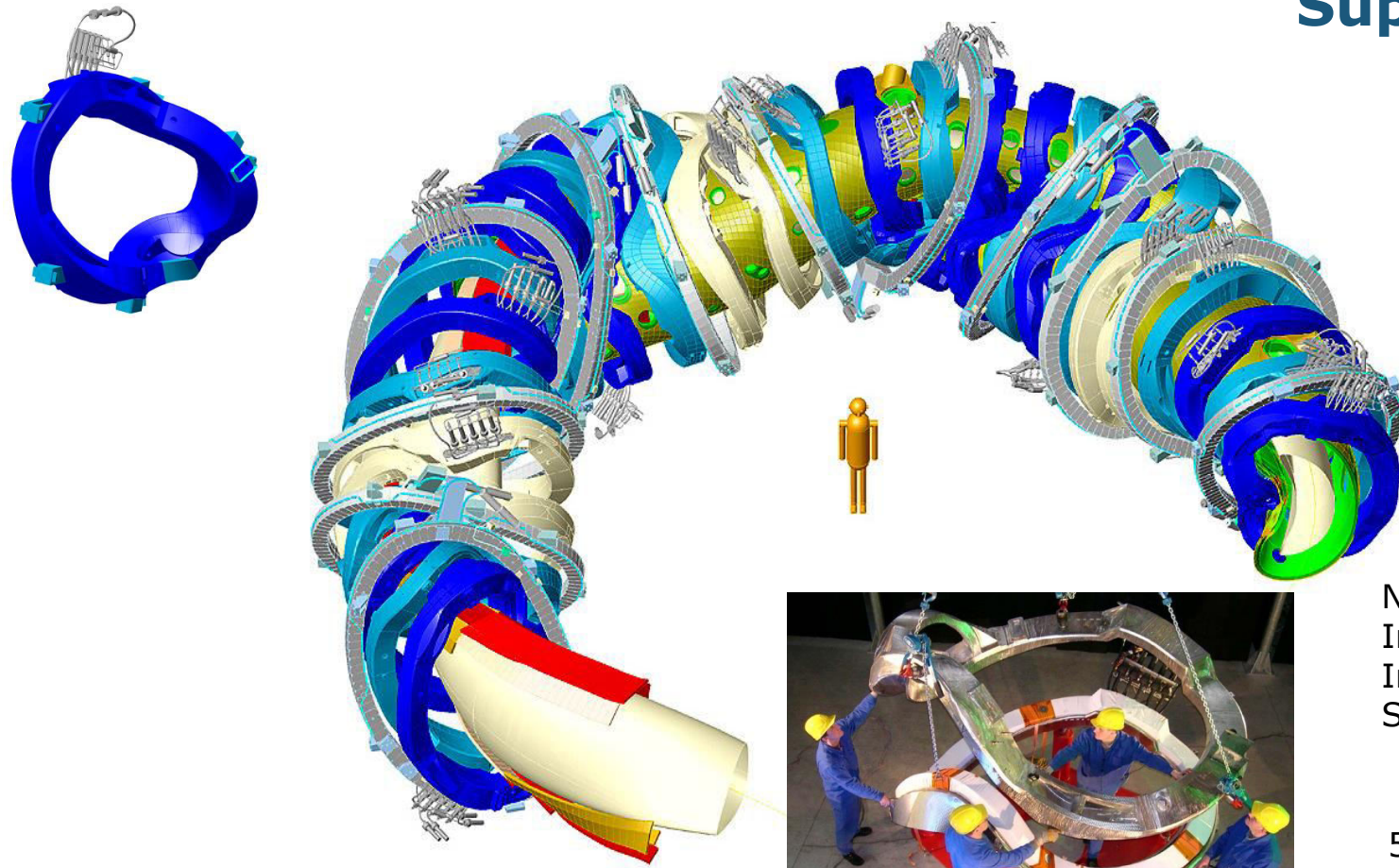


Parameter

Volume: 110 m³
Surface: 200 m²
Vacuum: < 10⁻⁸ mbar
Mass: 35 t
Tolerances < 2 mm



Stellarator



Superconducting Coils

Coils

NbTi superconductor (> 3.4 K)
Induction on axis: 2.5 T (< 3 T)
Induction at coil: 6.8 T at 17.8 kA
Stored magnetic energy: 600 MJ

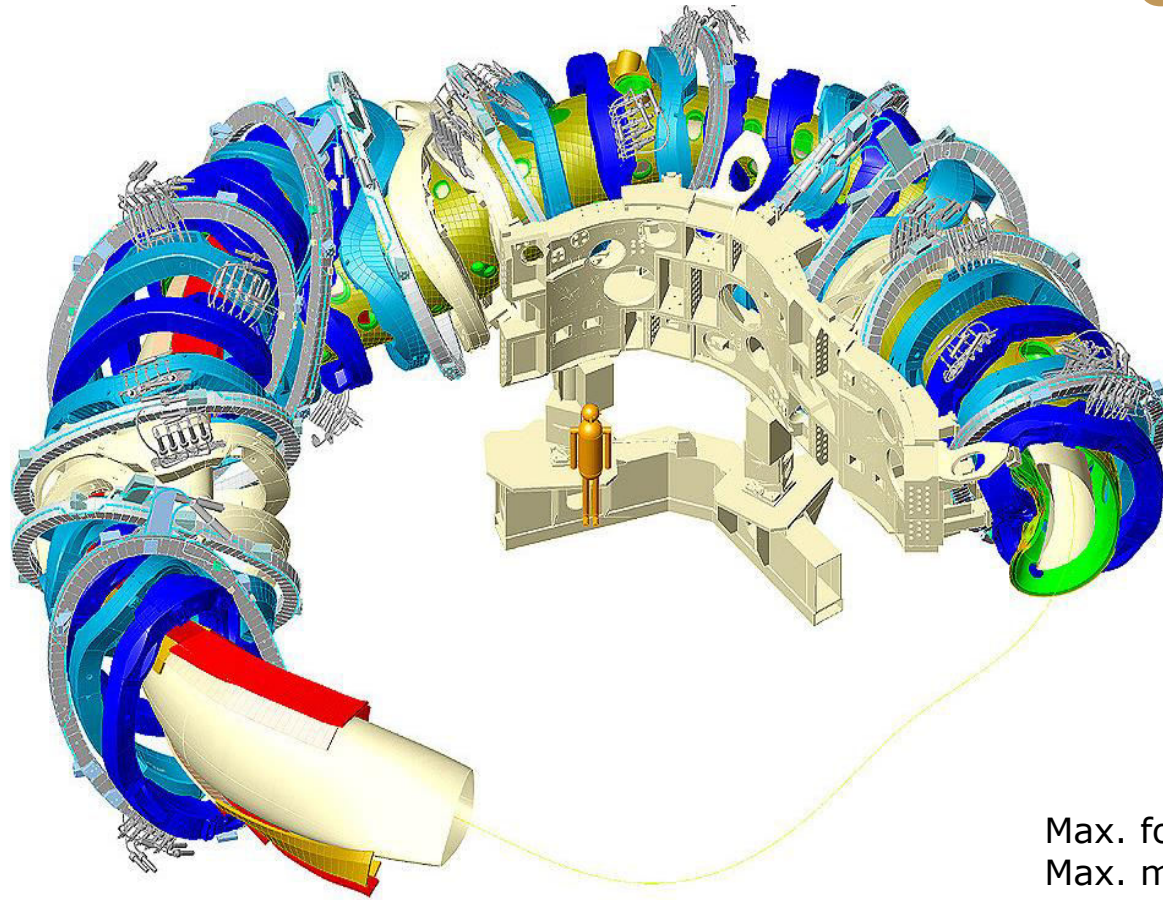
Parameter

50 non-planar coils, 5 types
20 planar coils, 2 types, variation
5 modules, 2 sym. halfmodules



Stellarator

Coil Support Structure



Parameter

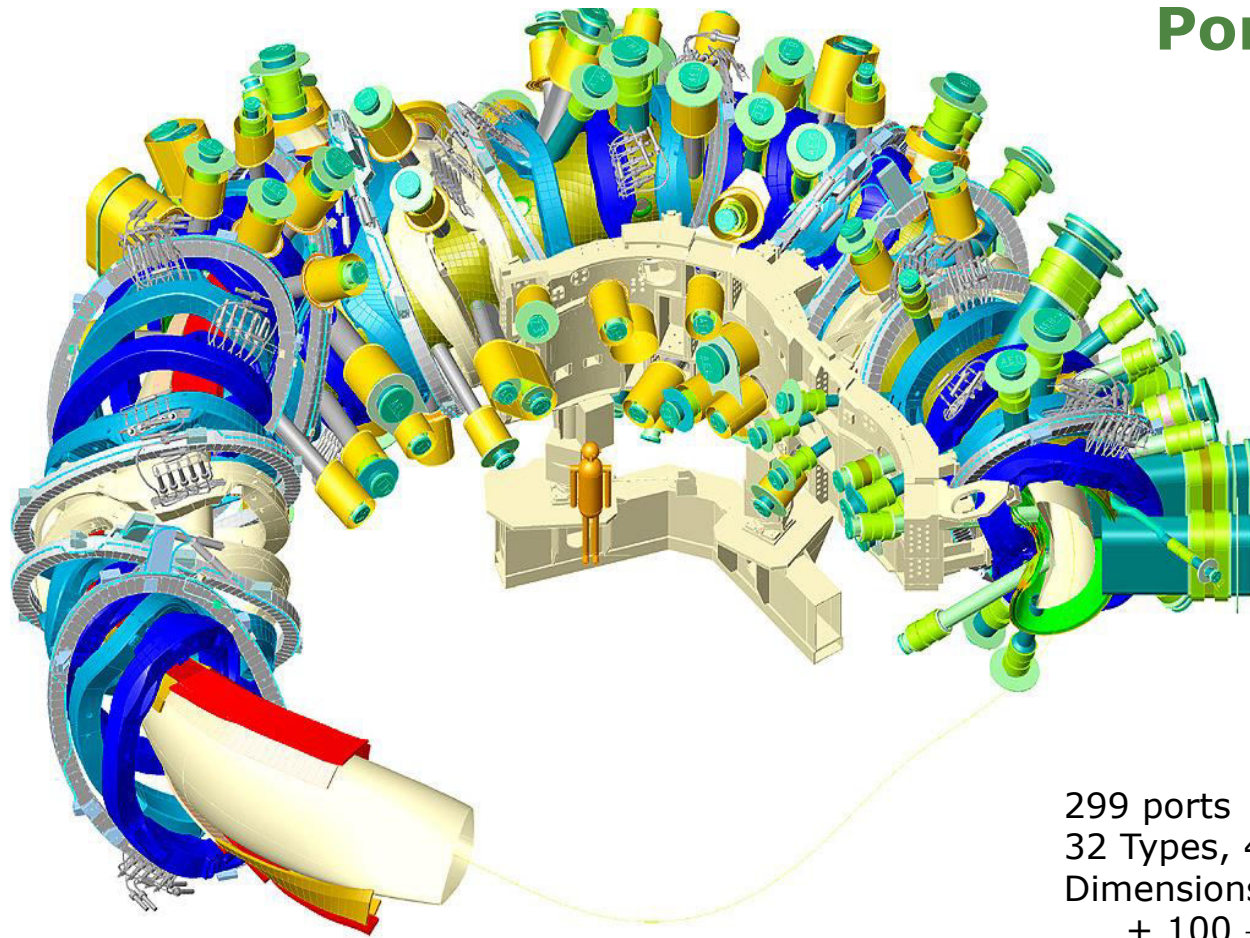
Max. force/coil: 3.6 MN

Max. moments: 0.8 MNm

2 supports/coil

Welded connections between coils

Stellarator

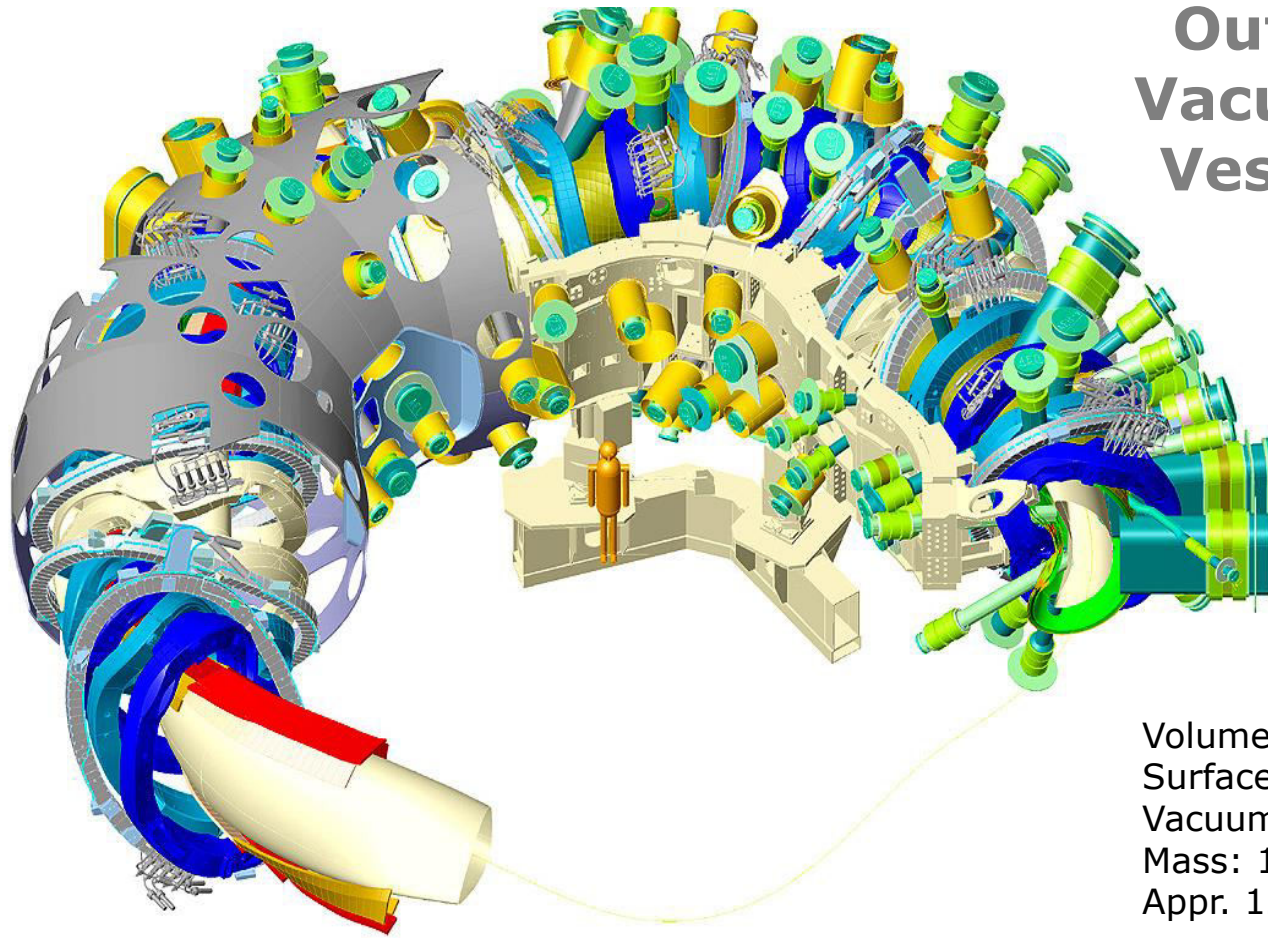


Ports

Parameter

299 ports
32 Types, 47 shapes
Dimensions
+ 100 → 400 mm
+ 150x400 → 400x1000 mm²

Stellarator



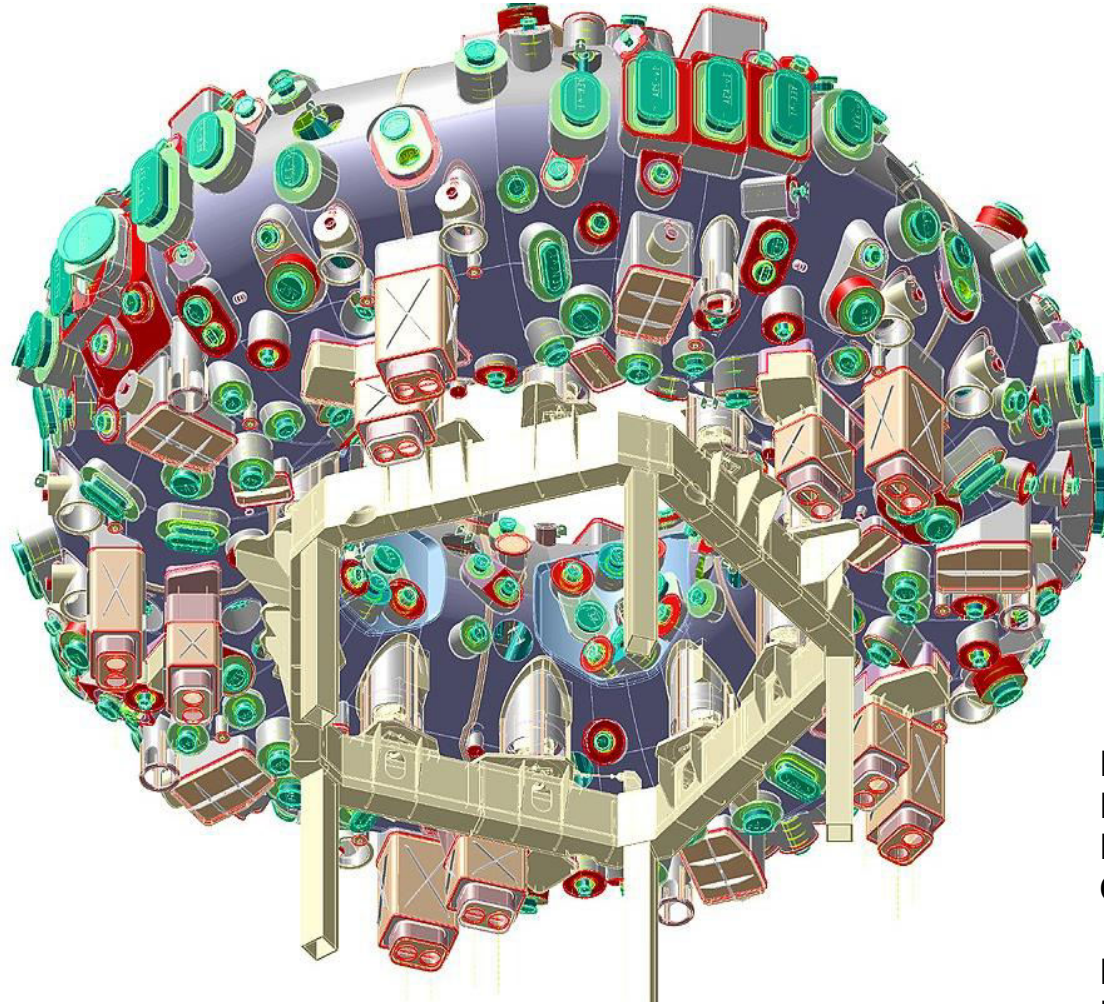
Outer Vacuum Vessel

Parameter

Volume: 525 m³
Surface: 480 m²
Vacuum: < 10⁻⁵ mbar
Mass: 150 t
Appr. 1200 openings

Thermal insulation on all warm surfaces of the cryostat

Stellarator



Schematic View

Parameter

Machine height: 4.5 m

Machine diameter: 16 m

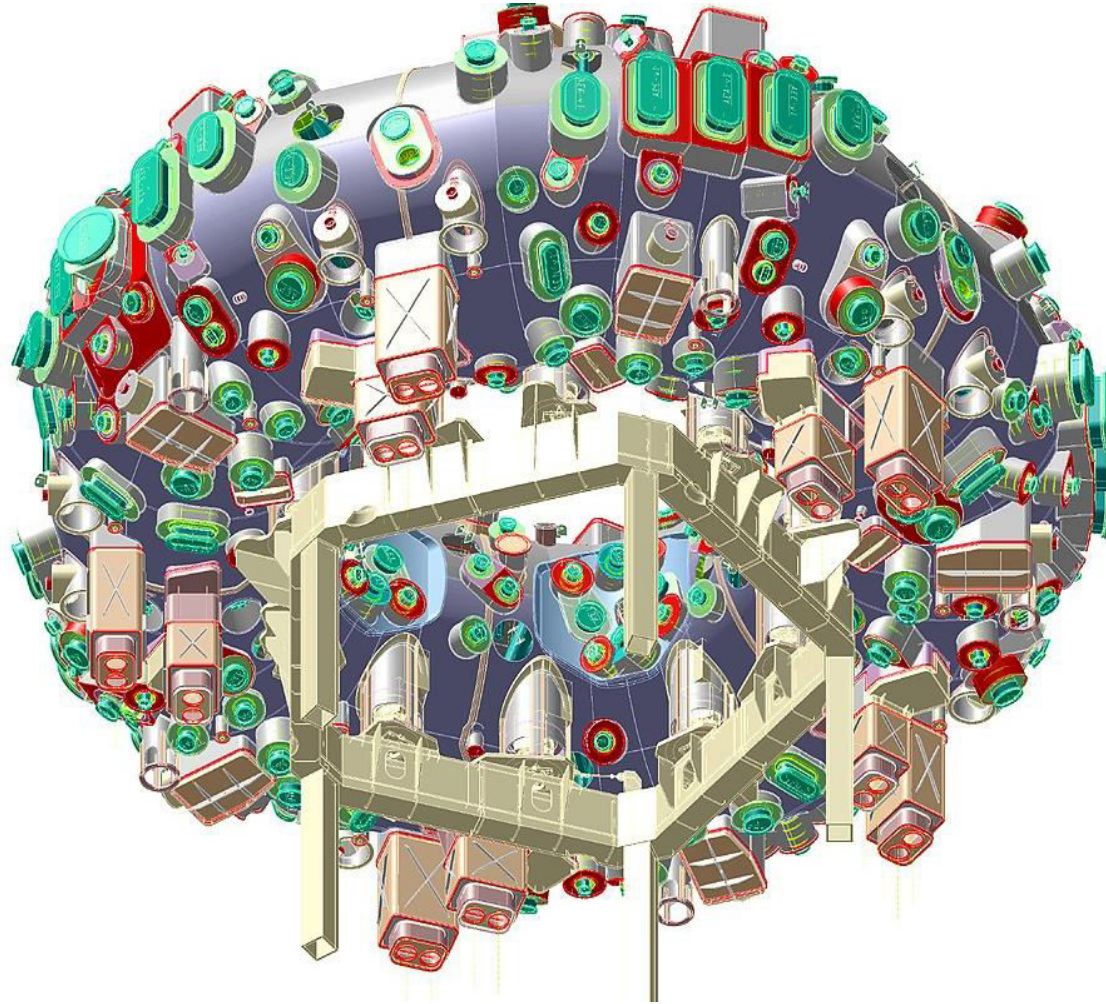
Machine mass: 725 t

Cold mass: 425 t

Heating power: 15 - 30 MW

Nominal pulse length: 30 min

Stellarator



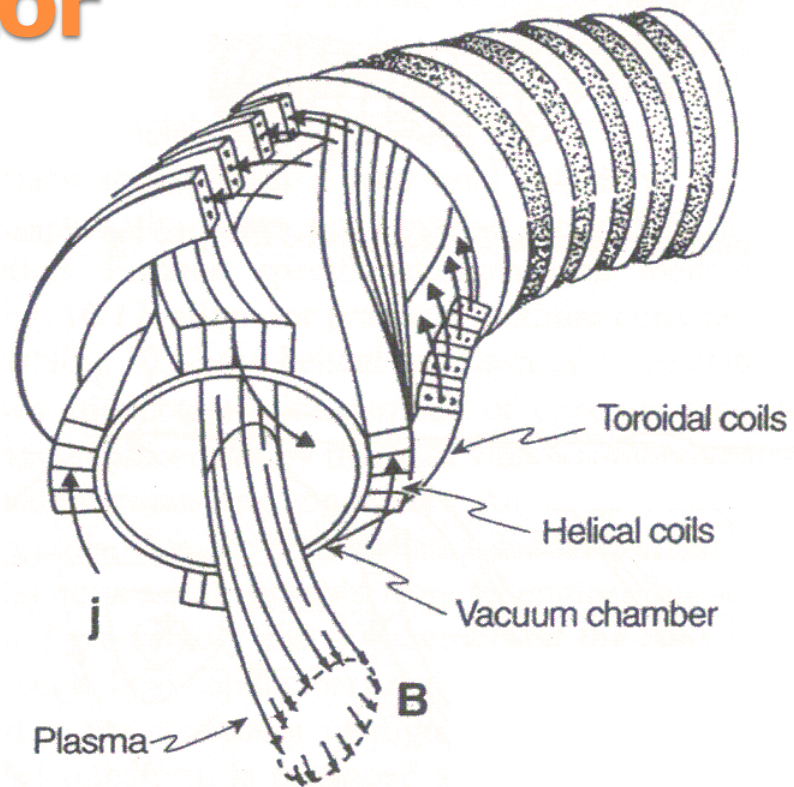
What a complex system it is!

Stellarator



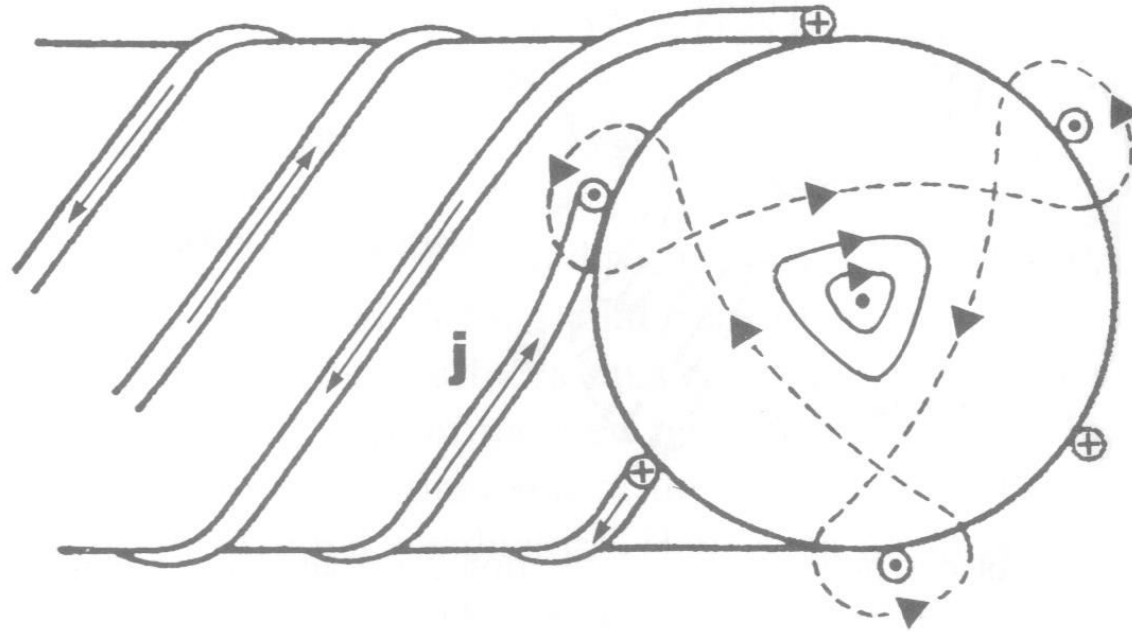
What a complex system it is!

Stellarator



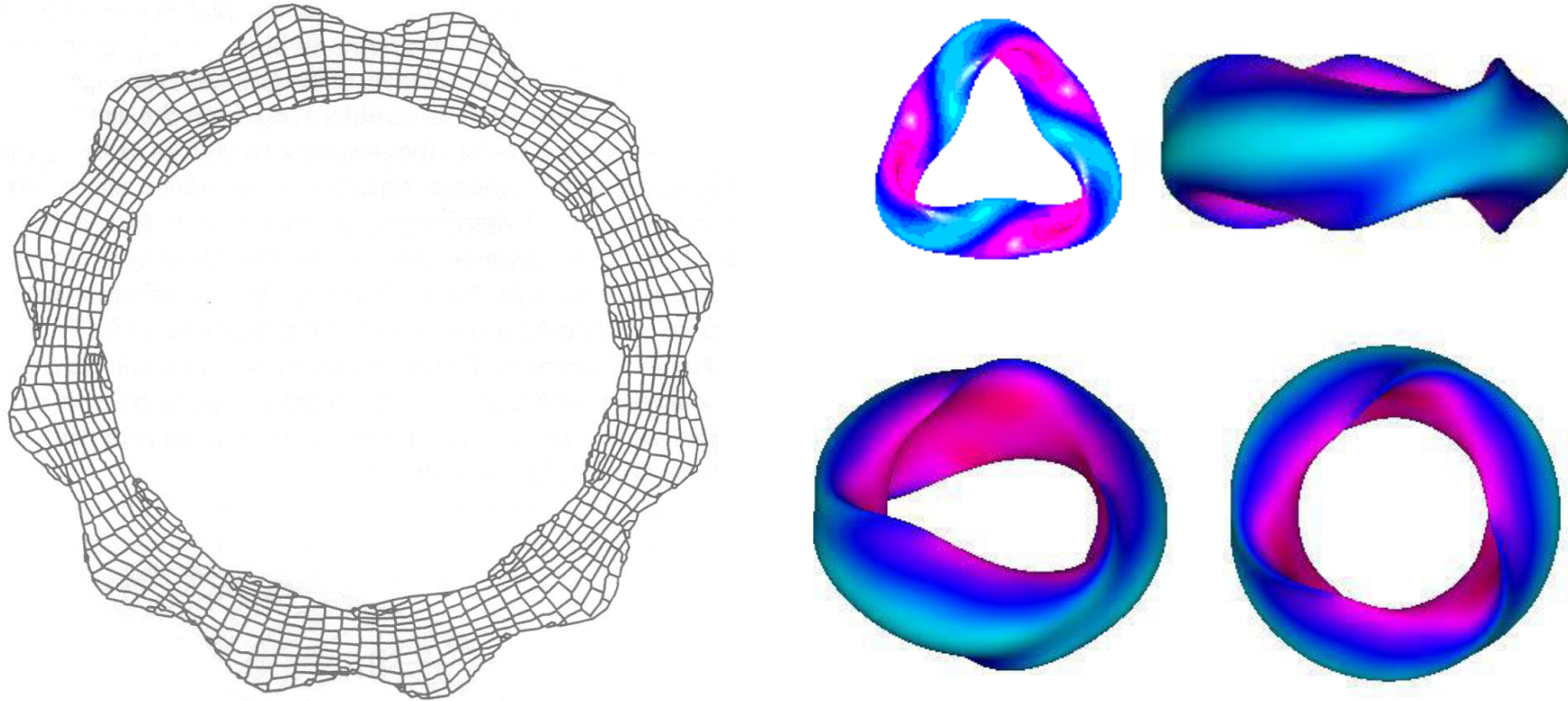
- The helical winding generates a toroidal field as well as a vertical field.
- To eliminate it, currents in adjacent helical windings of the same pitch flow in opposite directions canceling out one another's vertical fields and also their toroidal fields, on average. Thus, toroidal field coils are still required.

Stellarator



The magnetic surface for a stellarator with $l = 3$ pairs of helical coils of opposite currents

Stellarator



Complete magnetic flux surfaces:
The geometrical simplicity of axisymmetry lost

<http://www.ornl.gov/sci/fed/mhd/mhd.html>

A. A. Harms et al, "Principles of Fusion Energy", World Scientific (2000)

Stellarator

- **Inhomogeneity of the magnetic field**

- Due to the absence of a current in a stellarator, Ampere's law yields,

$$\nabla \times \vec{B} = \mu_0 \mathbf{J} \rightarrow \oint_s \frac{\vec{B}}{\mu_0} \cdot d\vec{s} = 0$$

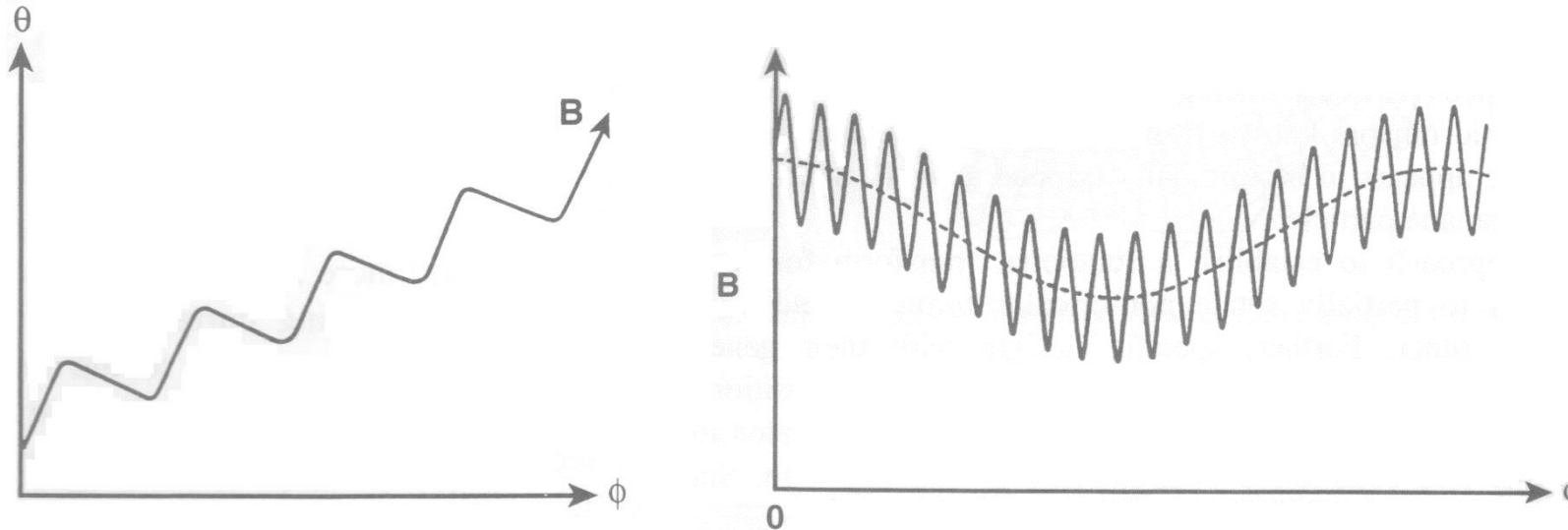
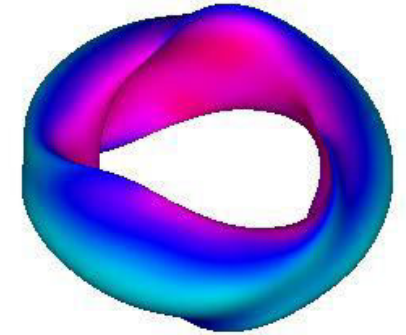
: The line integral of the poloidal component of the magnetic field vanishes along a contour s encircling the magnetic axis on each magnetic flux surface.

→ The poloidal field must change sign and magnitude along s . Each such so-called fundamental field period incrementally rotates the field lines in the poloidal direction.

- Curvature associated with torus geometry

Stellarator

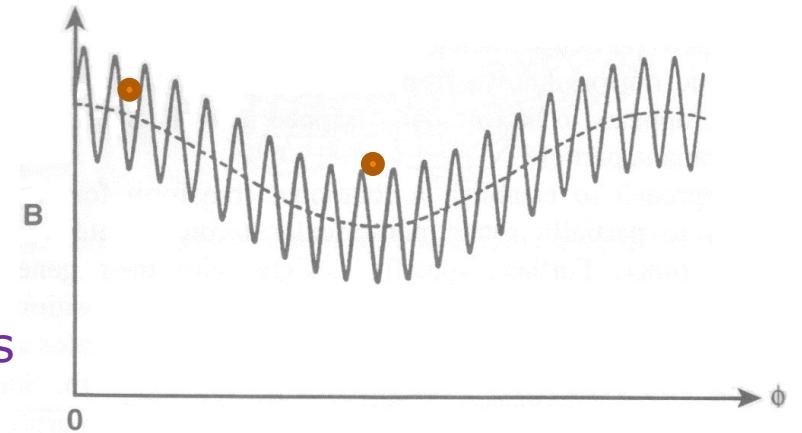
- Inhomogeneity of the magnetic field



- The deep and more frequent oscillations of \mathbf{B} are caused by the helical windings alternately carrying currents of different direction, and where the slow modulation of \mathbf{B} corresponds to the toroidal curvature.

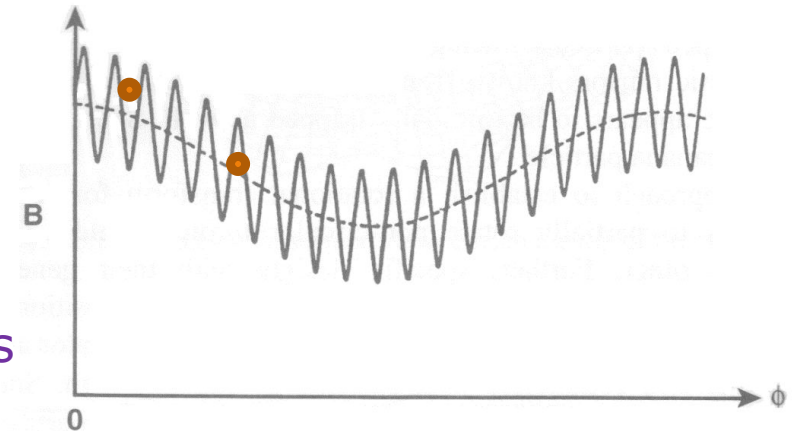
Stellarator

- **Inhomogeneity of the magnetic field**
 - Particle motions in this magnetic field configurations
 - (1) Circulating particles passing entirely around the torus without encountering a reflection
 - (2) Helically trapped particles reflected in the local mirrors of the helical field
 - (3) Toroidally trapped particles tracing banana orbits reflected in the toroidal magnetic mirrors
- Cf. Superbanana particle: a helically and toroidally trapped particle



Stellarator

- **Inhomogeneity of the magnetic field**
 - Particle motions in this magnetic field configurations
 - (1) Circulating particles passing entirely around the torus without encountering a reflection
 - (2) Helically trapped particles reflected in the local mirrors of the helical field
 - (3) Toroidally trapped particles tracing banana orbits reflected in the toroidal magnetic mirrors
- Cf. Superbanana particle: a helically and toroidally trapped particle



→ **Enhanced transport losses!**

Stellarator

- LHD achievement up to 2016 before D operation

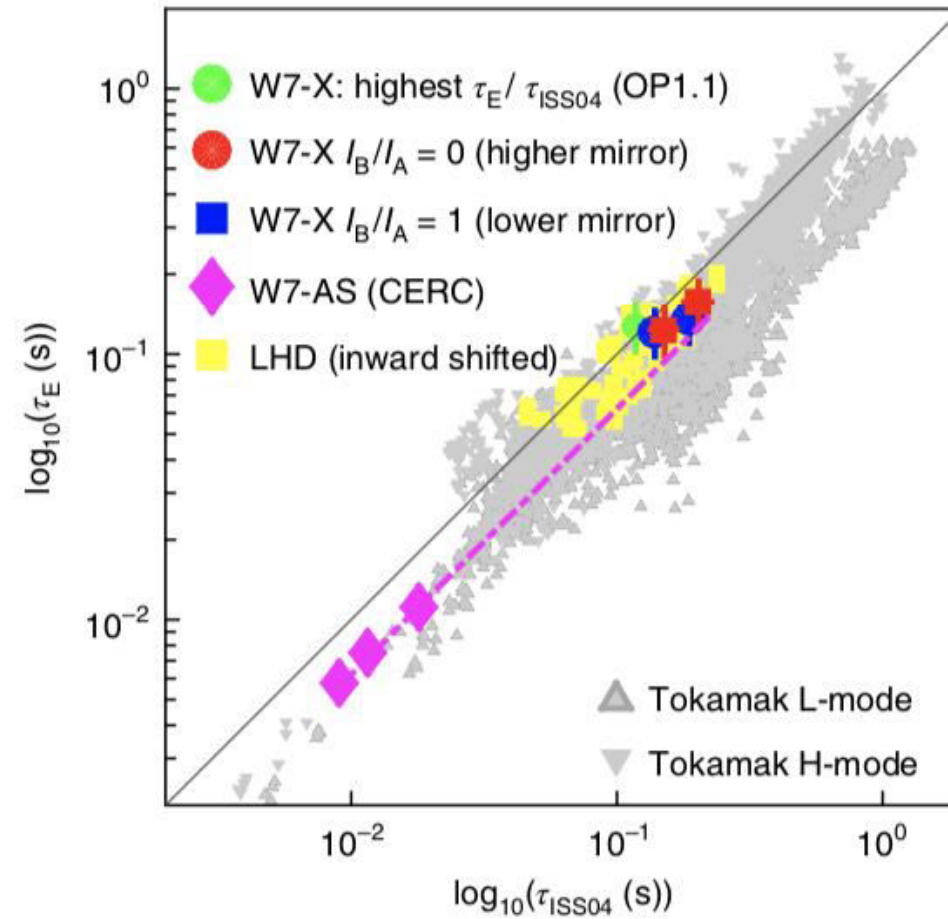
Plasma parameters	Achieved	Target	Fusion condition
Ion temperature	8.1 keV at $1 \times 10^{19} \text{m}^{-3}$	10 keV at $2 \times 10^{19} \text{m}^{-3}$	> 10 keV > $1 \times 10^{20} \text{m}^{-3}$
Electron temperature	20 keV at $2 \times 10^{18} \text{m}^{-3}$ 10 keV at $1.6 \times 10^{19} \text{m}^{-3}$	10 keV at $2 \times 10^{19} \text{m}^{-3}$	
Density	$1.2 \times 10^{21} \text{m}^{-3}$ with T_e of 0.25 keV	$4 \times 10^{20} \text{m}^{-3}$ with T_e of 1.3 keV	
Beta	5.1% at 0.425 T 4.1% at 1 T	5% at 1-2 T	> 5% at > 5 T
Steady-state operation	54min. 28sec (0.5 MW) (1keV, $4 \times 10^{18} \text{m}^{-3}$) 47min. 30sec. (1,2 MW) (2keV, $1 \times 10^{19} \text{m}^{-3}$)	1 hour (3 MW)	Steady-state (1 year)



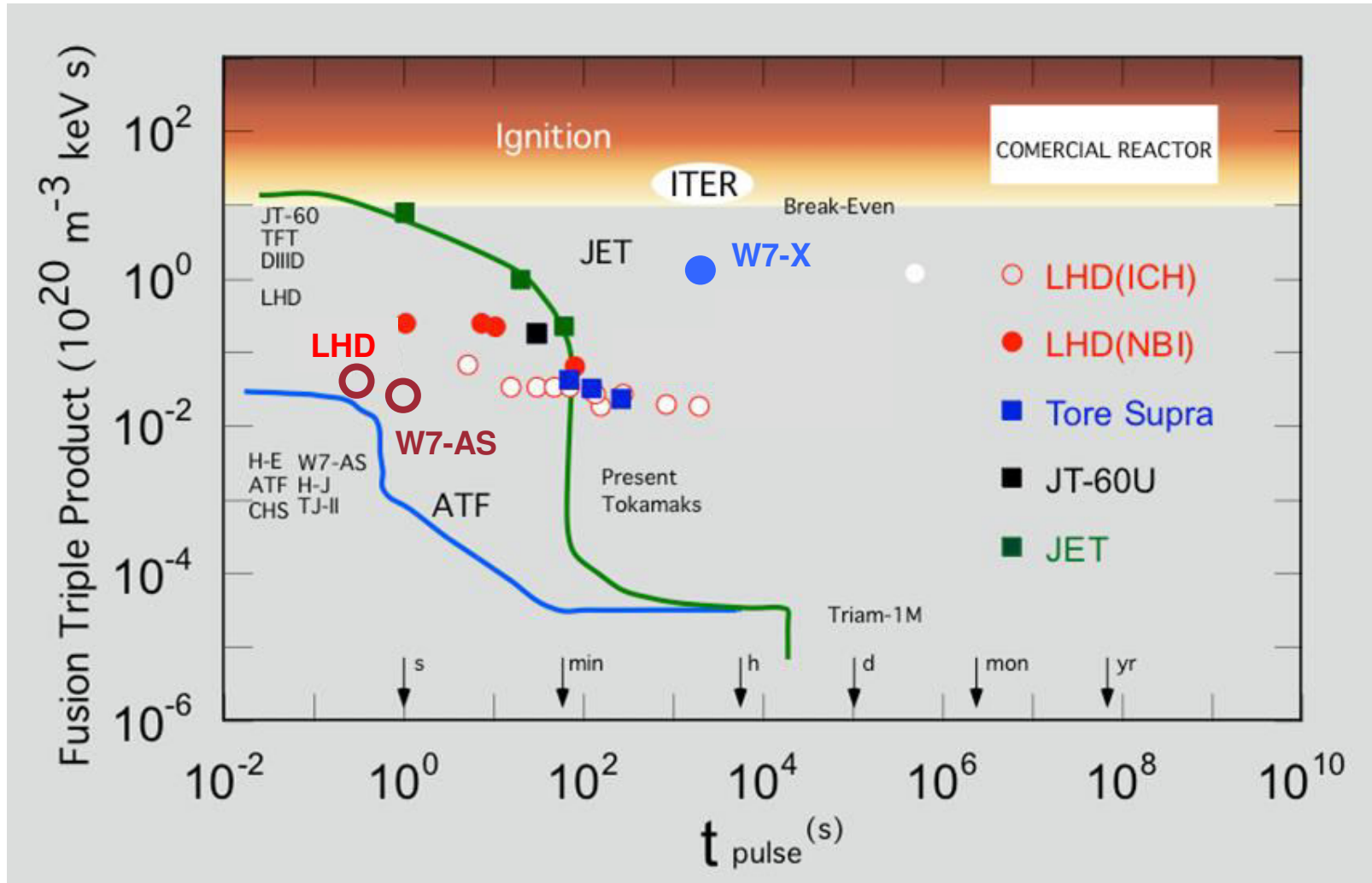
Tokamak .VS. Stellarator

	Advantage	Disadvantage
Tokamak	<ul style="list-style-type: none"> - Simple 2D structure, so relatively easy to analyze and fabricate the device - The most studied and successful up to now (mainstream in the roadmap to a feasible fusion reactor) 	<ul style="list-style-type: none"> - Need an external current drive (inductive or non-inductive) for plasma current generation & steady-state operation - Subject to plasma current-driven instabilities and disruptions
Stellarator	<ul style="list-style-type: none"> - No external current drive necessary, so inherently steady-state operation possible - Relatively free from plasma current-driven instabilities and disruptions 	<ul style="list-style-type: none"> - Complicated 3D structure, so difficult to analyse and fabricate the device - Large system size required with a high aspect ratio - Subject to large neoclassical transport at low collisionality - existence of bootstrap current

Tokamak .VS. Stellarator



Tokamak .VS. Stellarator



Introduction to Nuclear Fusion

Prof. Dr. Yong-Su Na

Plasma Equilibrium, Stability and Transport

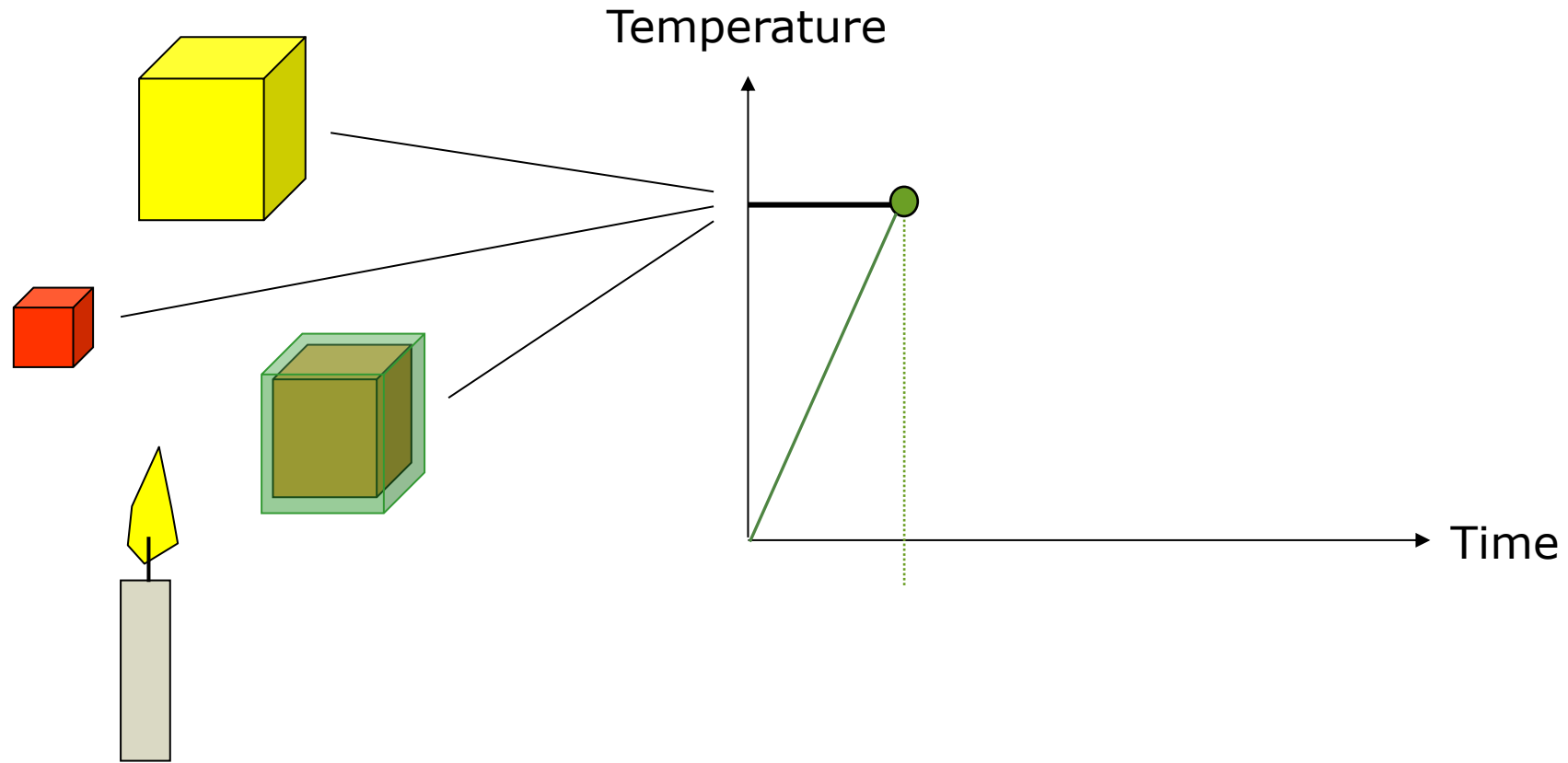


Tokamak
(magnetic pressure)

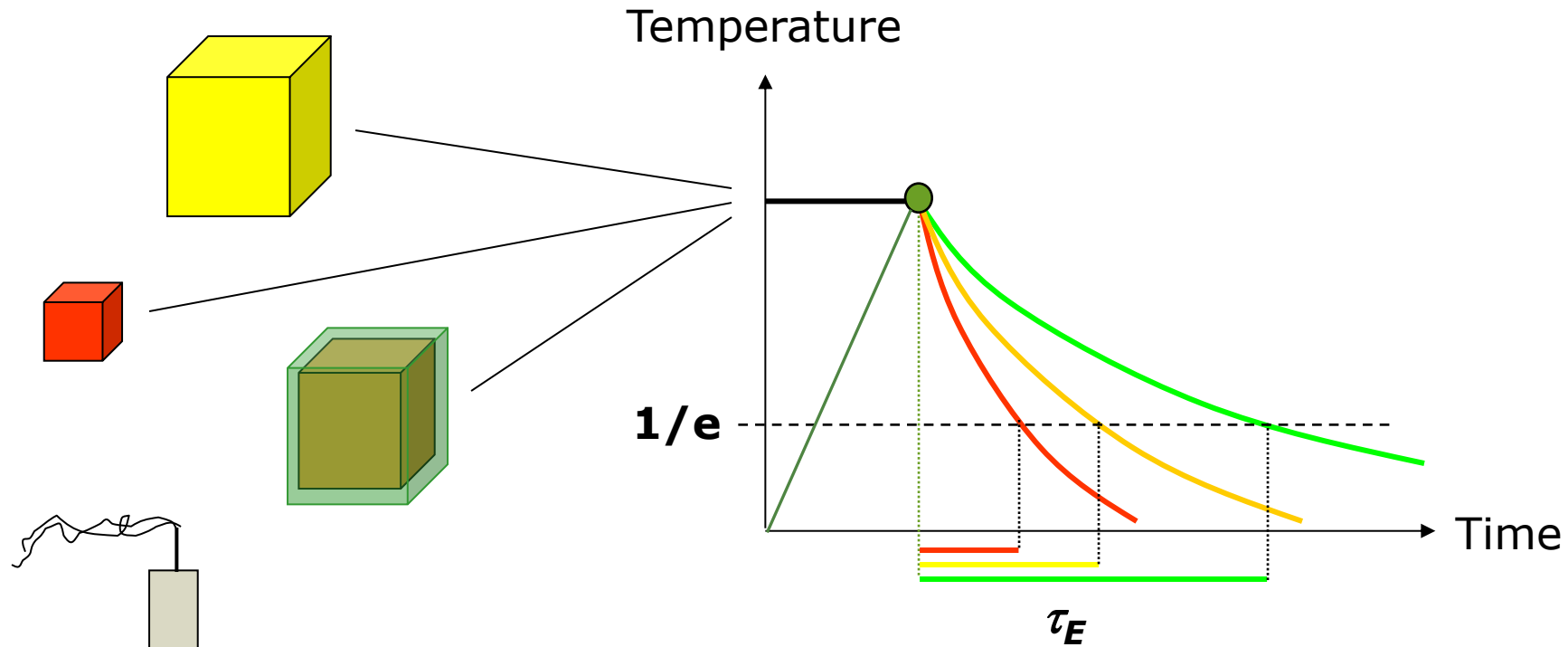


Plasma transport in a Tokamak

Energy Confinement Time



Energy Confinement Time



- τ_E is a measure of how fast the plasma loses its energy.
- The loss rate is smallest, τ_E largest if the fusion plasma is big and well insulated.

Tokamak Transport

• Transport Coefficients

$$\Gamma = -D\nabla n \quad : \text{Fick's law} \qquad D = \frac{(\Delta x)^2}{2\tau} \quad : \text{diffusion coefficient (m}^2\text{/s)}$$

$$q = -\kappa\nabla T \quad : \text{Fourier's law} \qquad D \sim v_{th}^2\tau \sim \frac{\lambda_m^2}{\tau}$$

Thermal diffusivity

$$\chi \equiv \frac{\kappa}{n} \approx D \approx \frac{(\Delta x)^2}{\tau} \approx \frac{a^2}{\tau_E} \quad \rightarrow \quad \tau_E \approx \frac{a^2}{\chi}$$

- Particle transport in fully ionised plasmas with magnetic field

$$D_{\perp} = \frac{\eta_{\perp} n \sum kT}{B^2}$$

Tokamak Transport

- **Classical Transport**

- Classical thermal conductivity (expectation): $\chi_i \sim 40\chi_e$
- Typical numbers expected: $\sim 10^{-4}$ m²/s
- Experimentally found: ~ 1 m²/s, $\chi_i \sim \chi_e$

Bohm diffusion (1946):
$$D_{\perp} = \frac{1}{16} \frac{kT_e}{eB}$$



David Bohm
(1917-1992)

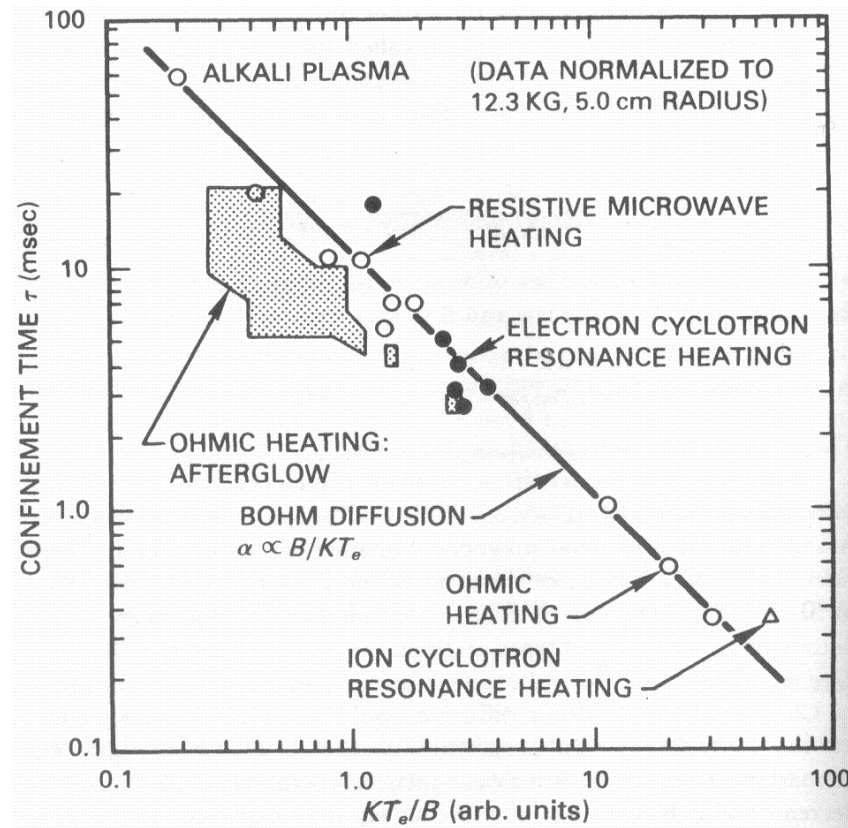


Aharonov-Bohm effect

Tokamak Transport

• Classical Transport

Bohm diffusion:
$$D_{\perp} = \frac{1}{16} \frac{kT_e}{eB}$$



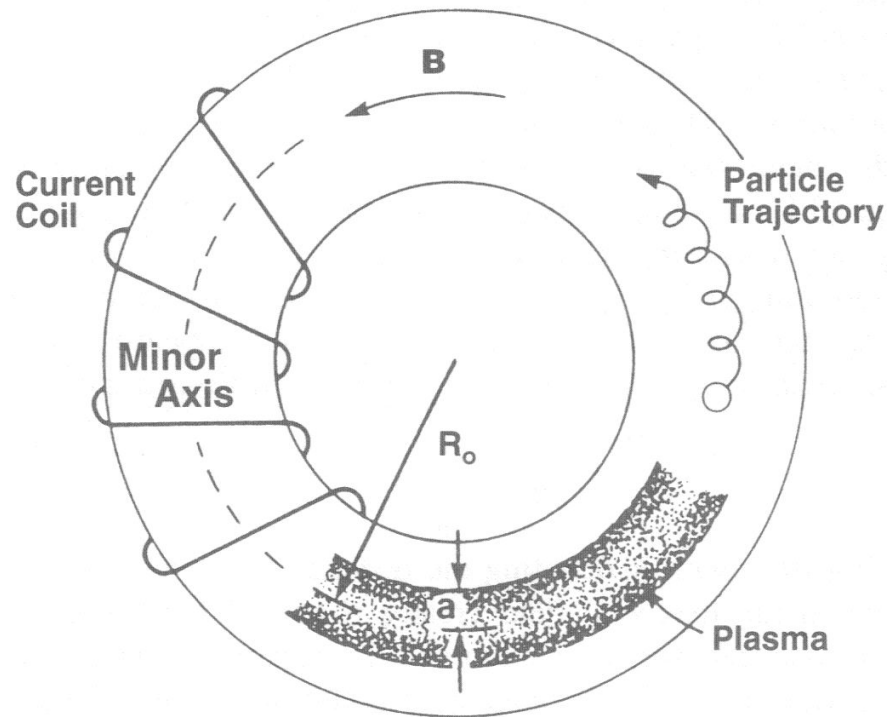
T_E in various types of discharges in the Model C Stellarator

F. F. Chen, "Introduction to Plasma Physics and Controlled Fusion" (2006)

Tokamak Transport

- Neoclassical Transport

- Major changes arise from toroidal effects characterised by inverse aspect ratio, $\epsilon = a/R_0$



Tokamak Transport

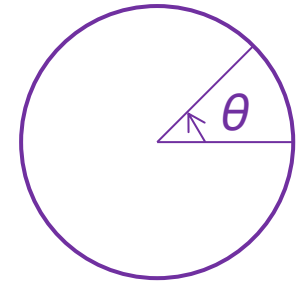
- Particle Trapping

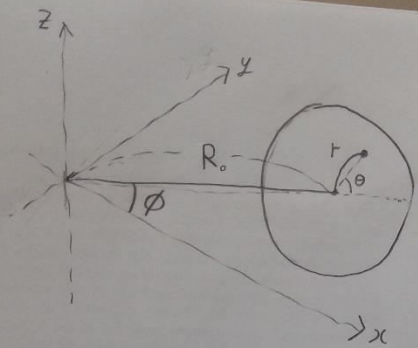
$$\nabla \cdot \vec{B} = 0$$

$$\Rightarrow \frac{1}{1 + \varepsilon \cos \theta} \left\{ \frac{1}{r} \frac{\partial}{\partial r} [r(1 + \varepsilon \cos \theta) B_r] + \frac{1}{r} \frac{\partial}{\partial \theta} [(1 + \varepsilon \cos \theta) B_\theta] + \frac{1}{r R_0} \frac{\partial (r B_\phi)}{\partial \phi} \right\} = 0$$

$$\Rightarrow B_\theta(r, \theta) = \frac{B_\theta^0(\theta = 0)}{1 + \varepsilon \cos \theta}$$

$$|B(r, \theta)| = |B_\theta(r, \theta) \hat{\theta} + B_\phi(r, \theta) \hat{\phi}| = \frac{B_0}{1 + \varepsilon \cos \theta}$$





$$\left(\begin{array}{l} \text{가정: } \frac{\partial}{\partial \phi} = 0 \\ B_r = 0 \\ J_r = 0 \end{array} \right)$$

$$\vec{r} = (R_0 + r \cos \theta) \cos \phi \hat{x} + (R_0 + r \cos \theta) \sin \phi \hat{y} + r \sin \theta \hat{z}$$

$$\frac{\partial \vec{r}}{\partial r} = \cos \theta \cos \phi \hat{x} + \cos \theta \sin \phi \hat{y} + \sin \theta \hat{z}$$

$$\frac{\partial \vec{r}}{\partial \theta} = -r \sin \theta \cos \phi \hat{x} - r \sin \theta \sin \phi \hat{y} + r \cos \theta \hat{z}$$

$$\frac{\partial \vec{r}}{\partial \phi} = -(R_0 + r \cos \theta) \sin \phi \hat{x} + (R_0 + r \cos \theta) \cos \phi \hat{y}$$

$$\Rightarrow \hat{r} = \cos \theta \cos \phi \hat{x} + \cos \theta \sin \phi \hat{y} + \sin \theta \hat{z}, \quad h_r = \left| \frac{\partial \vec{r}}{\partial r} \right| = 1$$

$$\hat{\theta} = -\sin \theta \cos \phi \hat{x} - \sin \theta \sin \phi \hat{y} + \cos \theta \hat{z}, \quad h_\theta = \left| \frac{\partial \vec{r}}{\partial \theta} \right| = r$$

$$\hat{\phi} = -\sin \phi \hat{x} + \cos \phi \hat{y}, \quad h_\phi = \left| \frac{\partial \vec{r}}{\partial \phi} \right| = R_0 + r \cos \theta$$

$$\Rightarrow \nabla \cdot \vec{A} = \frac{1}{h_r h_\theta h_\phi} \left[\frac{\partial}{\partial r} (h_\theta h_\phi A_r) + \frac{\partial}{\partial \theta} (h_r h_\phi A_\theta) + \frac{\partial}{\partial \phi} (h_r h_\theta A_\phi) \right]$$

$$\Rightarrow \nabla \cdot \vec{B} = \frac{1}{r(R_0 + r \cos \theta)} \left[\frac{\partial}{\partial r} (r(R_0 + r \cos \theta) B_r) + \frac{\partial}{\partial \theta} ((R_0 + r \cos \theta) B_\theta) + \frac{\partial}{\partial \phi} (r B_\phi) \right]$$

$$= 0$$

$$\left(\begin{array}{l} \text{Axisymmetric} \rightarrow \frac{\partial}{\partial \phi} = 0 \\ \vec{B} = B_\theta \hat{\theta} + B_\phi \hat{\phi} \rightarrow B_r = 0 \end{array} \right)$$

$$\Rightarrow \nabla \cdot \vec{B} = \frac{1}{r(R_0 + r \cos \theta)} \left[\frac{\partial}{\partial \theta} (R_0 + r \cos \theta) B_\theta \right] = 0$$

$$\Rightarrow B_\theta(r, \theta) = \frac{\text{const}(r)}{R_0 + r \cos \theta} = \frac{B_0(r, \frac{\pi}{2})}{1 + \epsilon \cos \theta} \quad (\epsilon \equiv \frac{r}{R_0})$$

1/2 전 Ampere's law $\nabla \times \vec{B} = \mu_0 \vec{J}$

$$\nabla \times \vec{A} = \frac{1}{h_r h_\theta h_\phi} \begin{vmatrix} h_r \hat{r} & h_\theta \hat{\theta} & h_\phi \hat{\phi} \\ \frac{\partial}{\partial r} & \frac{\partial}{\partial \theta} & \frac{\partial}{\partial \phi} \\ h_r A_r & h_\theta A_\theta & h_\phi A_\phi \end{vmatrix}$$

$$\vec{B} = B_\theta(r, \theta) \hat{\theta} + B_\phi(r, \theta) \hat{\phi}$$

$$\vec{J} = J_\theta(r, \theta) \hat{\theta} + J_\phi(r, \theta) \hat{\phi} \quad \text{이러}$$

$$\Rightarrow \nabla \times \vec{B} = \frac{1}{r(R_0 + r \cos \theta)} \begin{vmatrix} \hat{r} & r \hat{\theta} & (R_0 + r \cos \theta) \hat{\phi} \\ \frac{\partial}{\partial r} & \frac{\partial}{\partial \theta} & \frac{\partial}{\partial \phi} \quad (\because \text{Axisymmetric}) \\ 0 & r B_\theta & (R_0 + r \cos \theta) B_\phi \end{vmatrix}$$

$$= \mu_0 J_\theta(r, \theta) \hat{\theta} + \mu_0 J_\phi(r, \theta) \hat{\phi}$$

$$r \text{ 성분이 없으므로 } \frac{\partial}{\partial \theta} (R_0 + r \cos \theta) B_\phi = 0$$

$$\Rightarrow B_\phi(r, \theta) = \frac{\text{const}(r)}{R_0 + r \cos \theta} = \frac{B_\phi(r, \frac{\pi}{2})}{1 + \epsilon \cos \theta} \quad (\epsilon = \frac{r}{R_0})$$

$$\therefore \vec{B} = B_\theta(r, \theta) \hat{\theta} + B_\phi(r, \theta) \hat{\phi}$$

$$= \frac{1}{1 + \epsilon \cos \theta} \left[B_\theta(r, \frac{\pi}{2}) \hat{\theta} + B_\phi(r, \frac{\pi}{2}) \hat{\phi} \right]$$

$$\therefore |\vec{B}| = \frac{B_0}{1 + \epsilon \cos \theta} \quad (B_0 = \sqrt{(B_\theta(r, \frac{\pi}{2}))^2 + (B_\phi(r, \frac{\pi}{2}))^2})$$

$$= |\vec{B}(r, \frac{\pi}{2})|$$

\therefore Axisymmetric ($\frac{\partial}{\partial \phi} = 0$) 이고, \vec{B}, \vec{J} 의 r 성분이 없으면 $B = \frac{B_0(r)}{1 + \epsilon \cos \theta}$ 이다.

Tokamak Transport

• Particle Trapping

$$\nabla \cdot \vec{B} = 0$$

$$\Rightarrow \frac{1}{1 + \varepsilon \cos \theta} \left\{ \frac{1}{r} \frac{\partial}{\partial r} [r(1 + \varepsilon \cos \theta) B_r] + \frac{1}{r} \frac{\partial}{\partial \theta} [(1 + \varepsilon \cos \theta) B_\theta] + \frac{1}{rR_0} \frac{\partial (rB_\phi)}{\partial \phi} \right\} = 0$$

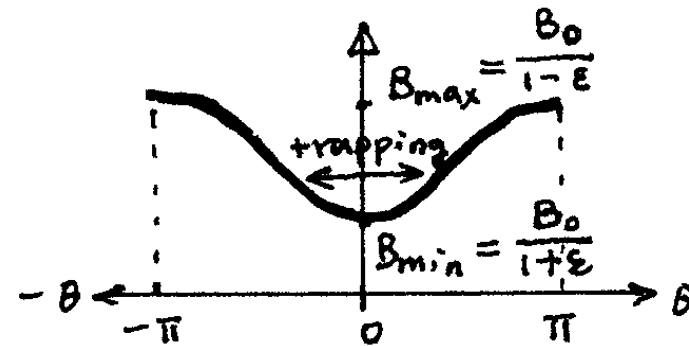
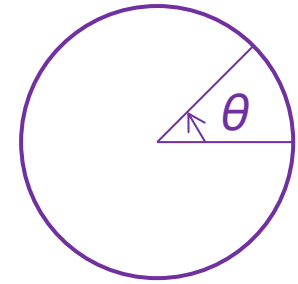
$$\Rightarrow B_\theta(r, \theta) = \frac{B_\theta^0(\theta = 0)}{1 + \varepsilon \cos \theta}$$

$$|B(r, \theta)| = |B_\theta(r, \theta) \hat{\theta} + B_\phi(r, \theta) \hat{\phi}| = \frac{B_0}{1 + \varepsilon \cos \theta}$$

- Condition for trapping of particles

$$\frac{(v_\parallel^2)_{\max}}{(v_\perp^2)_{\min}} = \left(\frac{v_\parallel^2}{v_\perp^2} \right)_{\text{mid-plane}} \leq \frac{B_{\max}}{B_{\min}} - 1 = \frac{1 - \varepsilon}{1 + \varepsilon} - 1 = \frac{2\varepsilon}{1 - \varepsilon} \sim 2\varepsilon$$

$$\Rightarrow v_\parallel^2 \leq 2\varepsilon v_\perp^2$$



Tokamak Transport

• Particle Trapping

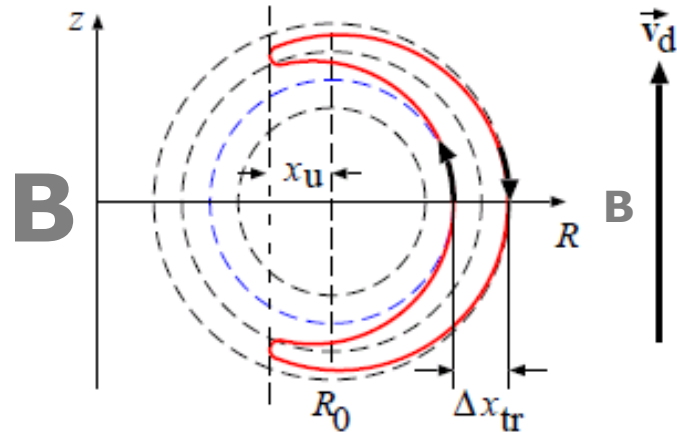
- Particle trapping by magnetic mirrors
trapped particles with banana orbits
untrapped particles with circular orbits

- Trapped fraction:
$$f_{trap} = \sqrt{1 - \frac{1}{R_m}} = \sqrt{1 - \frac{B_{min}}{B_{max}}} = \sqrt{1 - \frac{1 - \epsilon}{1 + \epsilon}} = \sqrt{\frac{2\epsilon}{1 + \epsilon}}$$

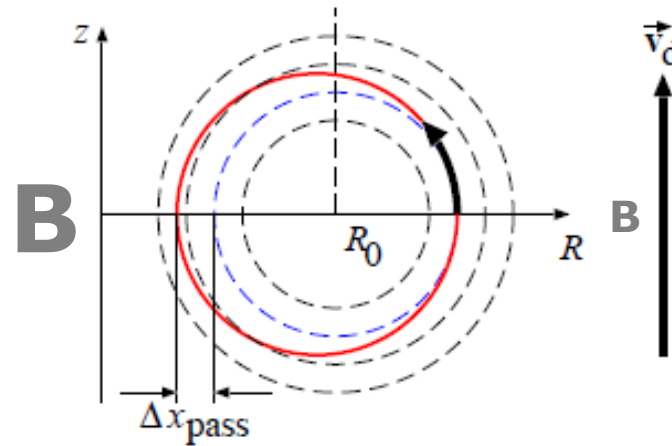
for a typical tokamak, $\epsilon \sim 1/3 \rightarrow f_{trap} \sim 70\%$

Tokamak Transport

• Particle Trapping



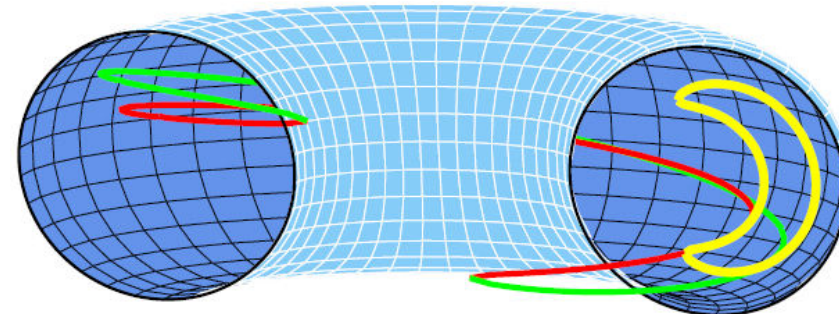
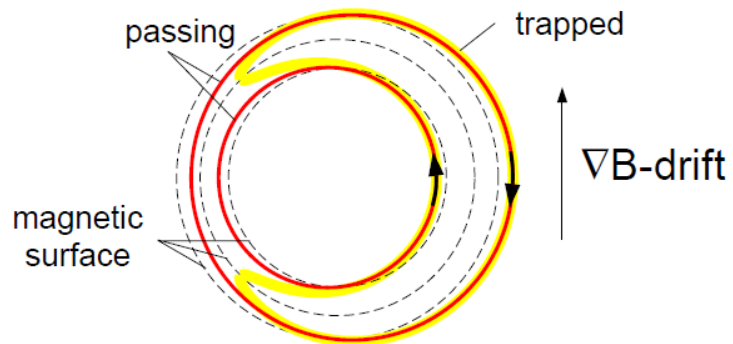
trapped particles



passing particles

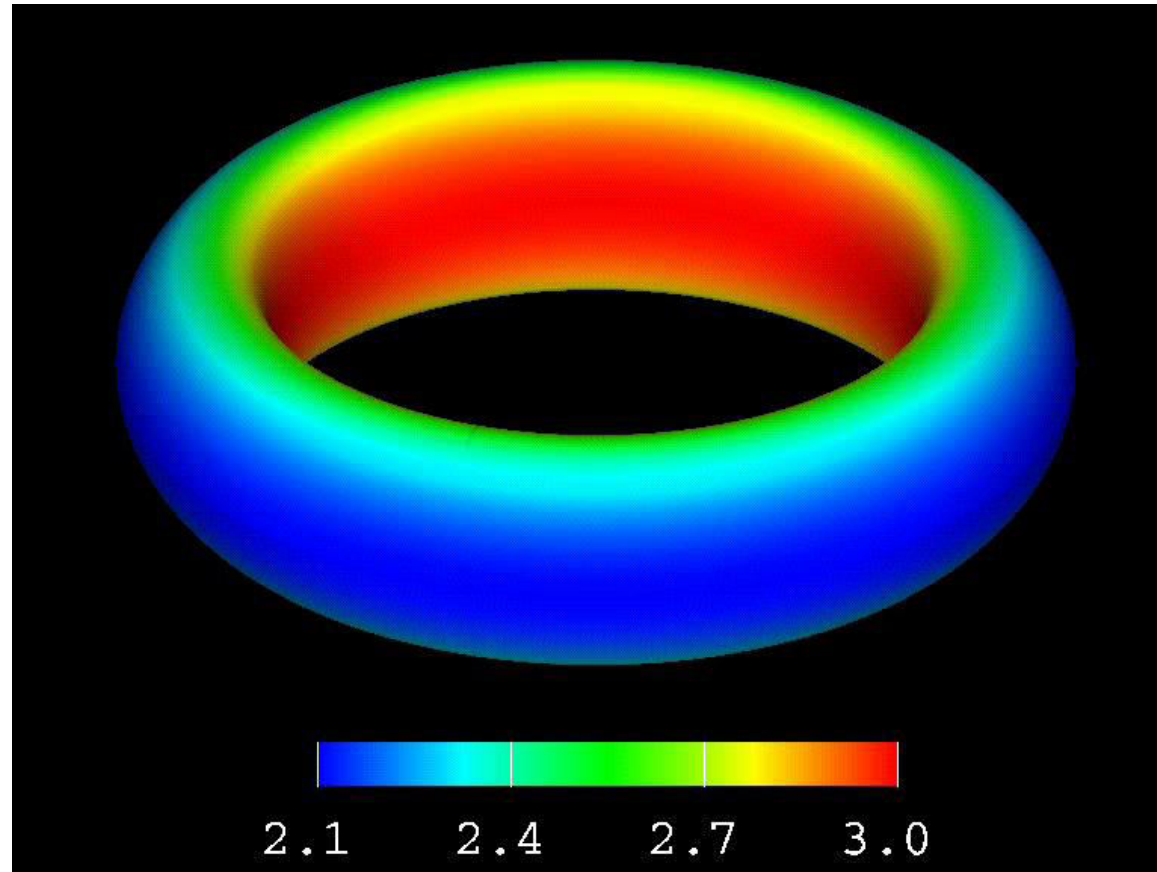
$$\mathbf{v}_{D,\nabla B} = \pm \frac{1}{2} v_{\perp} r_L \frac{\mathbf{B} \times \nabla B}{B^2}$$

$$\mathbf{v}_{D,R} = \frac{mv_{\parallel}^2}{qB_0^2} \frac{\mathbf{R}_0 \times \mathbf{B}_0}{R^2}$$



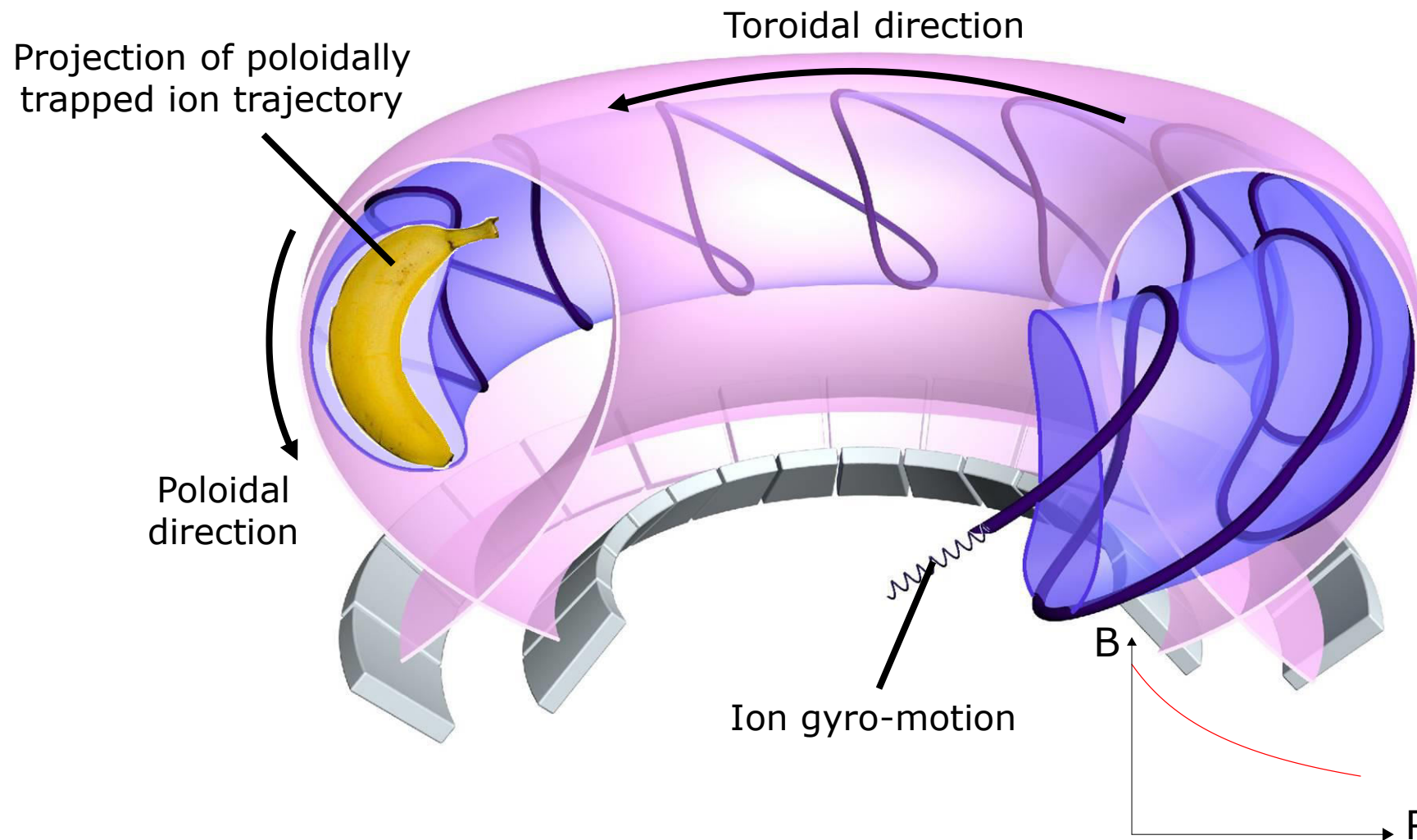
Tokamak Transport

- Particle Trapping



Tokamak Transport

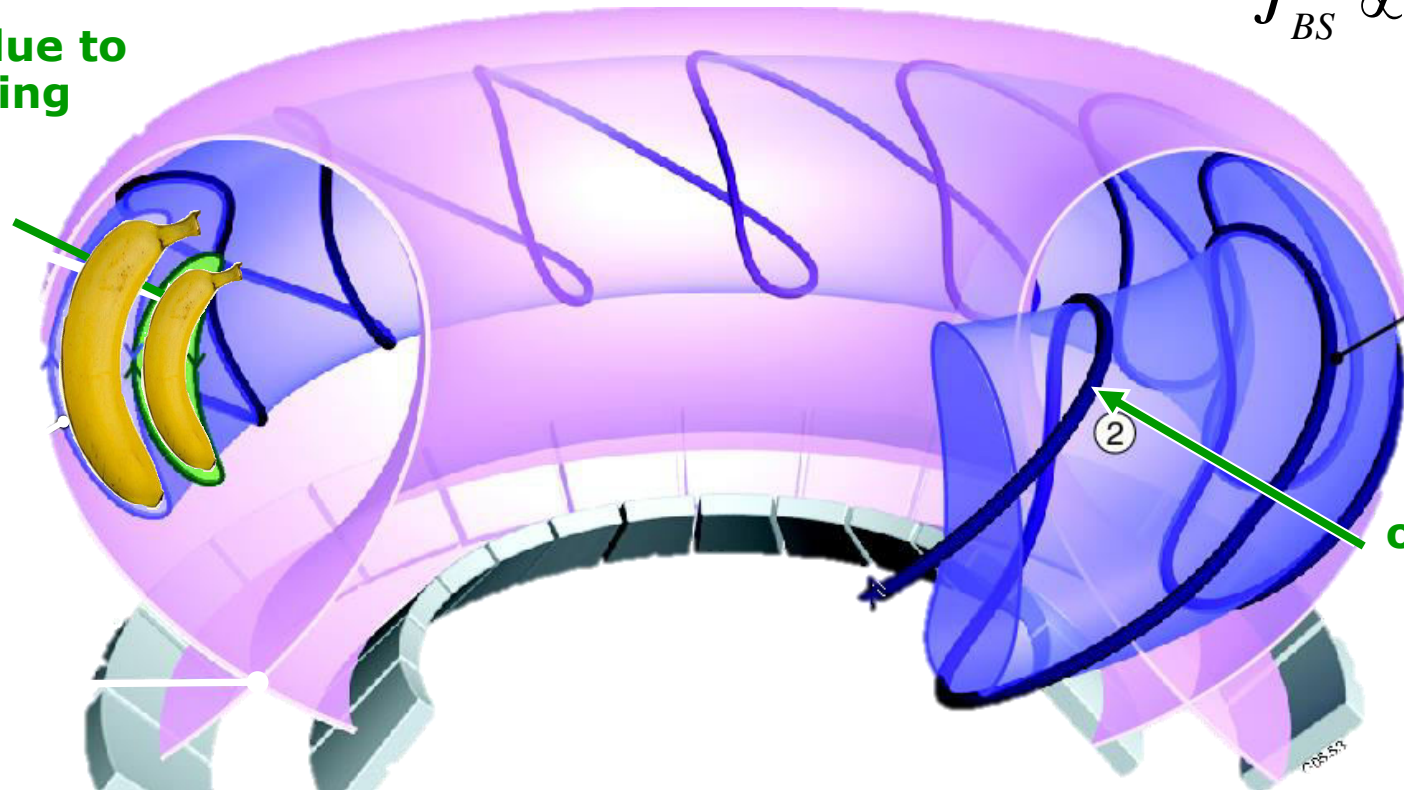
- Neoclassical Bootstrap current



Tokamak Transport

- Neoclassical Bootstrap current

Currents due to neighbouring bananas largely cancel



$$J_{BS} \propto \nabla p$$

orbits tighter where field stronger

- More & faster particles on orbits nearer the core (green .vs. blue) lead to a net "banana current".
- This is transferred to a helical bootstrap current via collisions.

Tokamak Transport

• Neoclassical Bootstrap current

야후! | 도움말 | 로그인

통합검색 통합사전

YAHOO! KOREA 통합사전

bootstrap

검색

통합사전 **NEW** 영어사전 일어사전 백과사전 국어사전 한자사전

영어사전

bootstrap [bú:tsræp]  PLAY  단어장에 추가

1. (편상화의) 손잡이 가죽.
2. <재귀용법으로> 노력하여 [자기]를 어떤 상태로 되게 하다.
3. 자동(식)의; 자급(自給)의; 자력의.

[▶ 영어사전 더보기](#)

- Named after the reported ability of Baron von Munchausen to lift himself by his bootstraps (Raspe, 1785)
- Suggested with 'Alice in Wonderland' in mind where the heroine managed to support herself in the air by her shoelaces.

Tokamak Transport

• Bootstrap

MEANING:

verb tr.: To help oneself with one's own initiative and no outside help.

noun: Unaided efforts.

adjective: Reliant on one's own efforts.

ETYMOLOGY:

While pulling on bootstraps may help with putting on one's boots, it's impossible to lift oneself up like that. Nonetheless the fanciful idea is a great visual and it gave birth to the idiom "to pull oneself up by one's (own) bootstraps", meaning to better oneself with one's own efforts, with little outside help. It probably originated from the tall tales of Baron Münchhausen who claimed to have lifted himself (and his horse) up from the swamp by pulling on his own hair.

In computing, booting or bootstrapping is to load a fixed sequence of instructions in a computer to initiate the operating system.

Earliest documented use: 1891.1



Baron Münchhausen lifting himself up from the swamp by his own hair
Illustrator: Theodor Hosemann

Tokamak Transport

- **Bootstrap**

“I was still a couple of miles above the clouds when it broke, and with such violence I fell to the ground that I found myself stunned, and in a hole nine fathoms under the grass, when I recovered, hardly knowing how to get out again. Looking down, I observed that I had on a pair of boots with exceptionally sturdy straps. Grasping them firmly, I pulled with all my might. Soon I had hoist myself to the top and stepped out on terra firma without further ado.”

- With acknowledgement to R. E. Raspe, *Singular Travels, Campaigns and Adventures of Baron Munchausen*, 1786. Edition edited by J. Carswell. London: The Cresset Press, 1948. Adapted from the story on p. 22(???)

Tokamak Transport

- Neoclassical Bootstrap current

Diffusion Driven Plasma Currents and Bootstrap Tokamak

by R. J. UKAEA Res the usual toroidal coordinates. Then in the regime of low collision frequency and in the absence of any driving electric field, steady state diffusion is accompanied by a toroidal current density of magnitude $\frac{R}{}$

$$j = -A \left(\frac{r}{R} \right)^{1/2} \frac{1}{B_\theta} \frac{dp}{dr} \quad (1)$$

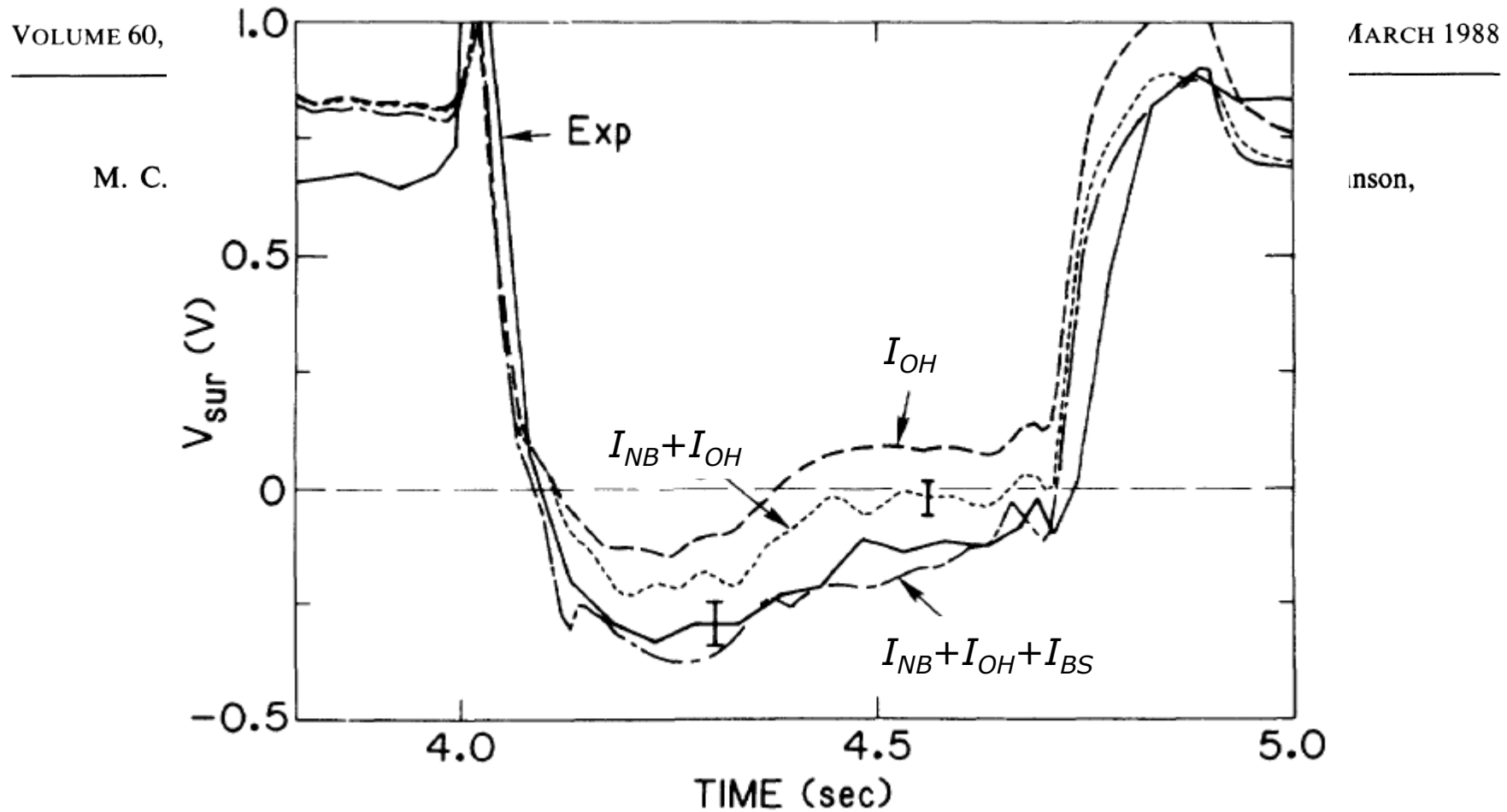
In toroid
ment
toroid
the m
to mag
currer
of Tokamak machine which operates in a steady state, unlike present pulsed designs.

where A is a coefficient whose value depends on the exact collision operator but is of order unity, and p is the plasma pressure.



Tokamak Transport

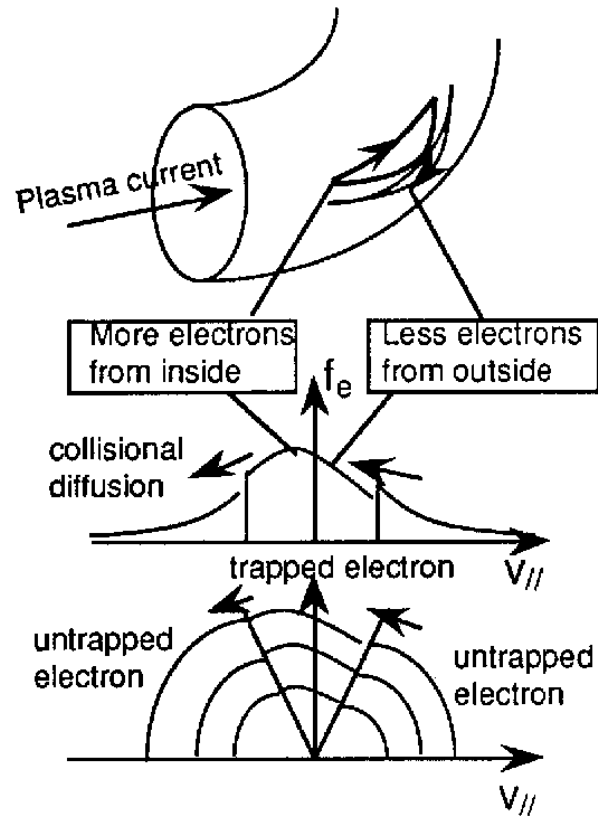
- Neoclassical Bootstrap current



Tokamak Transport

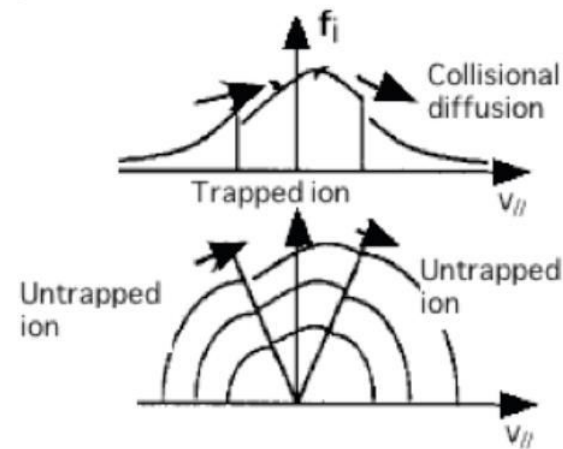
- **Neoclassical Bootstrap current**

- Trapped-electron orbits and schematics of the velocity distribution function in a collisionless tokamak plasma



Small Coulomb collision smooths the gap and causes particle diffusion in the velocity space.

Collisional pitch angle scattering at the trapped-untrapped boundary produces unidirectional parallel flow/momentum input and is balanced by the collisional friction force between electrons and ions.



Tokamak Transport

- Neoclassical Bootstrap current

- Bootstrap current fraction

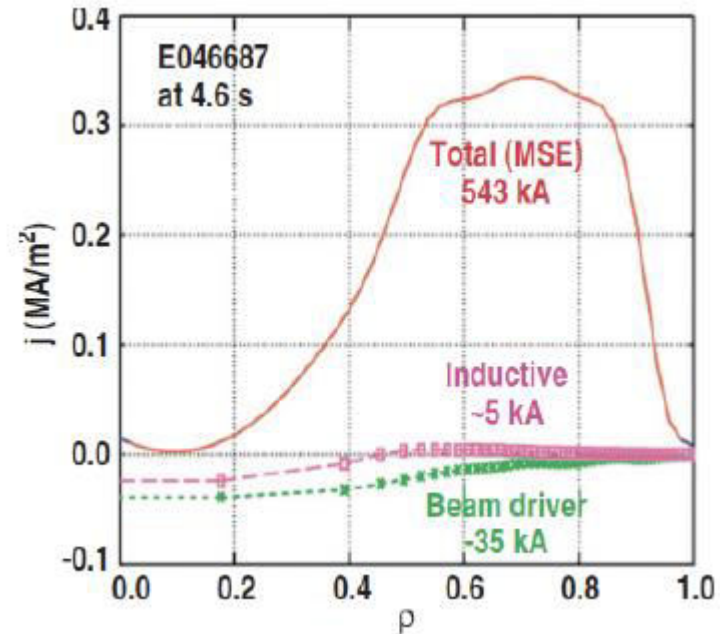
$$f_B(r) \equiv \frac{J_B}{J_\phi} \approx -1.18G\varepsilon^{1/2}\beta_p \sim \varepsilon^{1/2}\beta_p \qquad \beta_p = \frac{\langle p \rangle}{B_p^2 / 2\mu_0}$$
$$G(r) = (\ln n + 0.04 \ln T)' / (\ln r B_\theta)'$$

- In high- β tokamak, $\beta_p \sim 1/\varepsilon$, implying that $f_B \sim 1/\varepsilon^{1/2} \gg 1$:
The bootstrap current can theoretically overdrive the total current
- No obvious "anomalous" degradation of J_B due to micro-turbulence
- The bootstrap current is capable of being maintained in steady state without the need of an Ohmic transformer or external current drive.
This is indeed a favourable result as it opens up the possibility of steady state operation without the need for excessive amounts of external current drive power.
- This is critical since bootstrap current fractions on the order of $f_B > 0.7$ are probably required for economic viability of fusion reactors.

Tokamak Transport

- 100% bootstrap discharges

Y. Takase, IAEA FEC 1996, S. Coda, IAEA FEC 2008

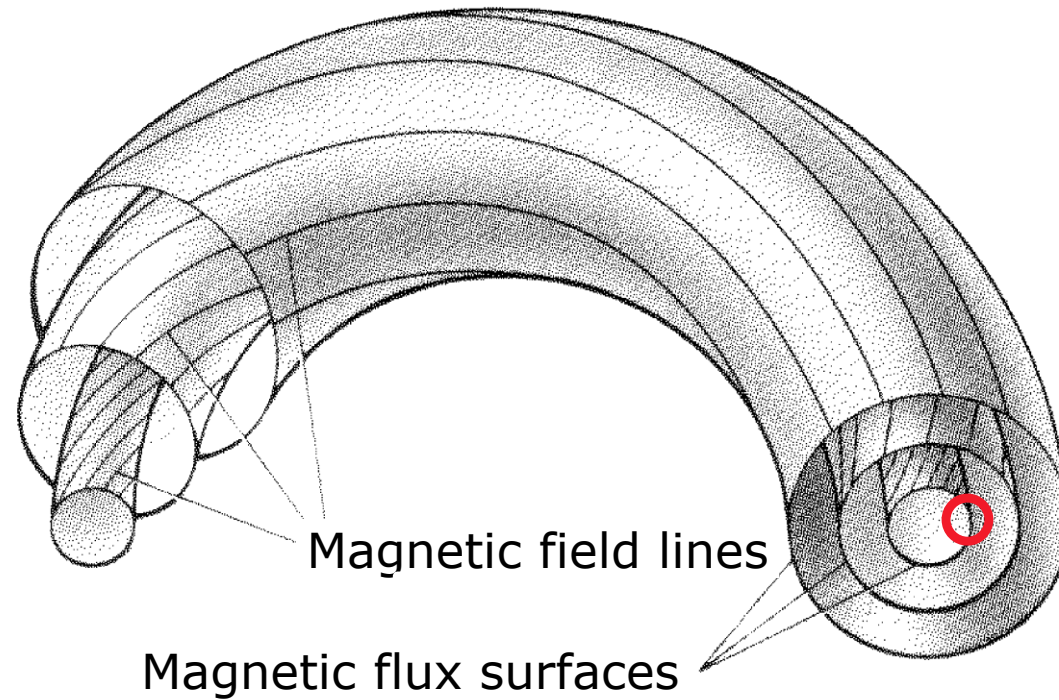


Tokamak Transport

• Particle Trapping

- Collisional excursion across flux surfaces
untrapped particles: $2r_g$ ($2r_{Li}$)

$$D = \frac{(\Delta x)^2}{2\tau} \quad : \text{diffusion coefficient (m}^2/\text{s)}$$

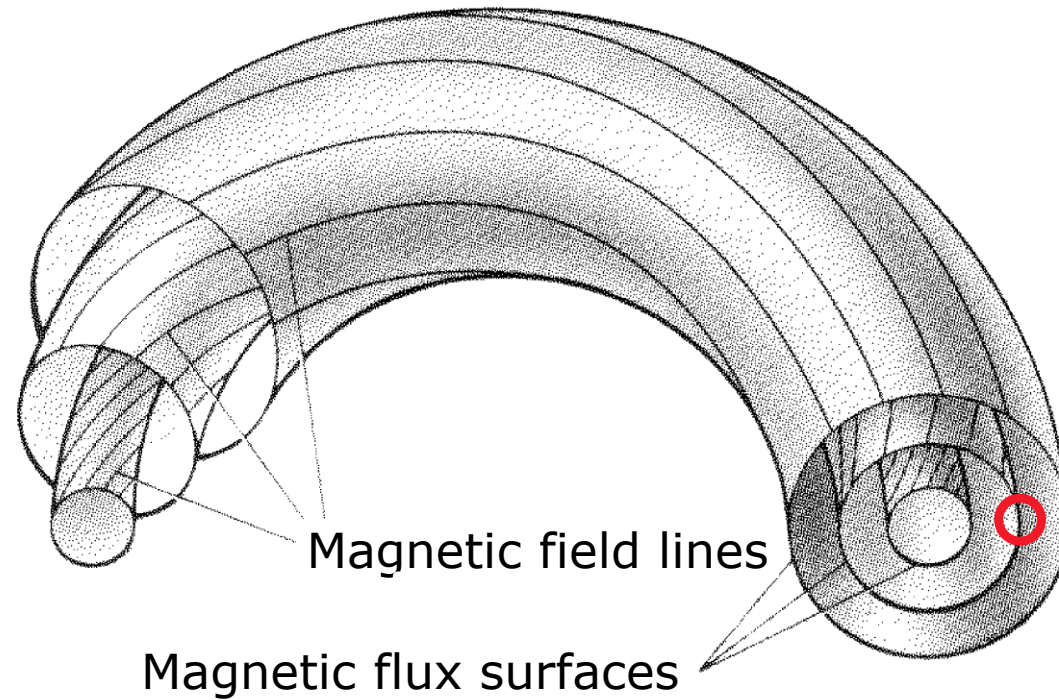


Tokamak Transport

• Particle Trapping

- Collisional excursion across flux surfaces
untrapped particles: $2r_g$ ($2r_{Li}$)

$$D = \frac{(\Delta x)^2}{2\tau} \quad : \text{diffusion coefficient (m}^2/\text{s)}$$



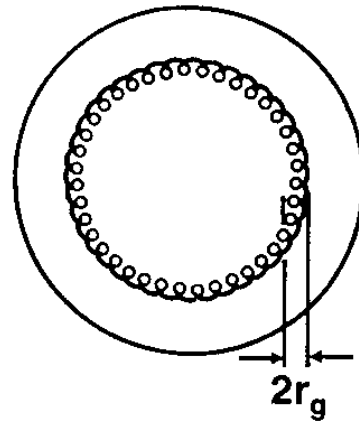
Tokamak Transport

• Particle Trapping

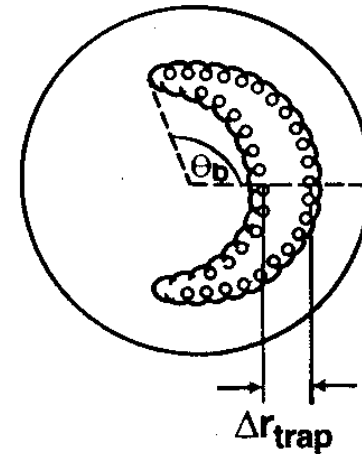
- Collisional excursion across flux surfaces

untrapped particles: $2r_g$ ($2r_{Li}$)

trapped particles: $\Delta r_{trap} \gg 2r_g$ – enhanced radial diffusion
across the confining magnetic field



Untrapped



Trapped

- If the fraction of trapped particle is large, this leakage enhancement constitutes a substantial problem in tokamak confinement.

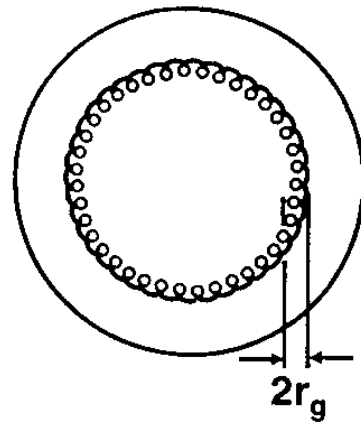
Tokamak Transport

• Particle Trapping

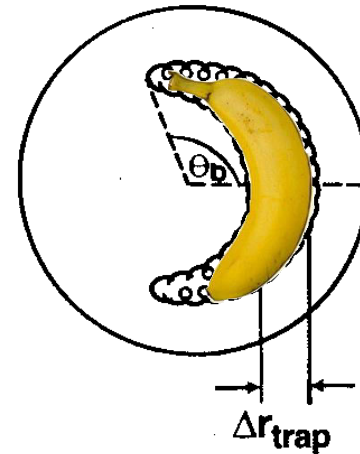
- Collisional excursion across flux surfaces

untrapped particles: $2r_g$ ($2r_{Li}$)

trapped particles: $\Delta r_{trap} \gg 2r_g$ – enhanced radial diffusion
across the confining magnetic field



Untrapped



Trapped

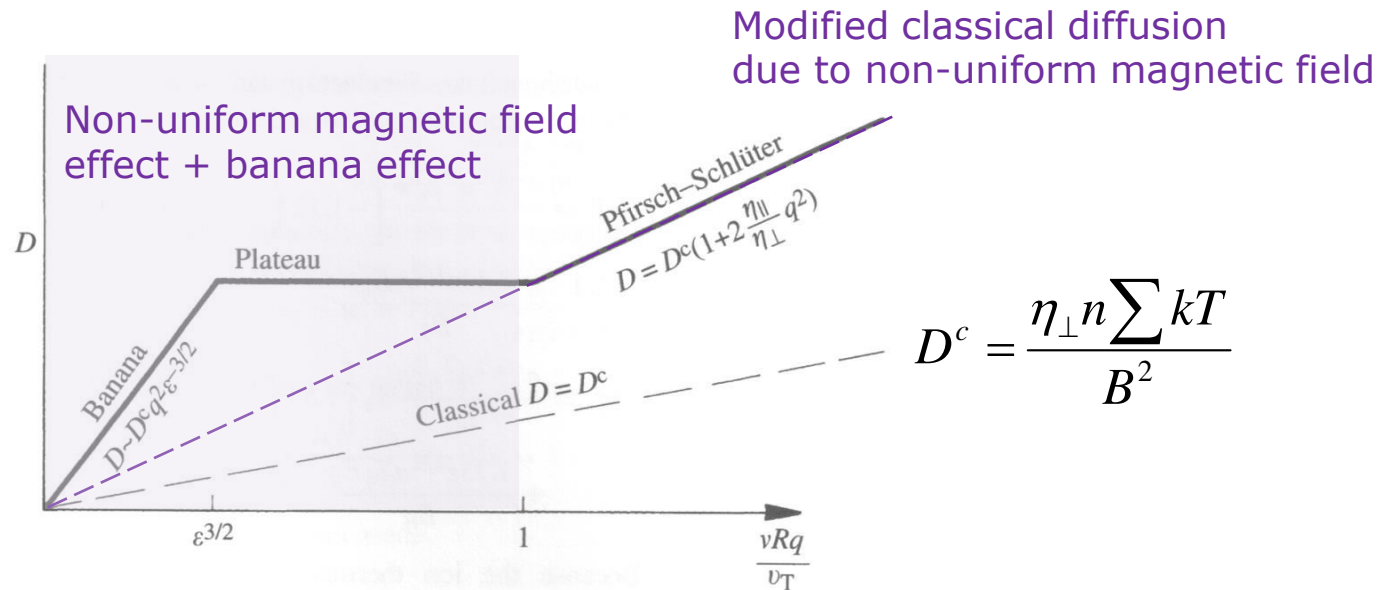
- If the fraction of trapped particle is large, this leakage enhancement constitutes a substantial problem in tokamak confinement.

Tokamak Transport

$$\Gamma = -D\nabla n \approx -\frac{(\Delta r)^2}{\tau} \nabla n : \text{Fick's law}$$

• Neoclassical Transports

- May increase D , χ up to two orders of magnitude:
 - χ_i 'only' wrong by factor 3-5
 - D , χ_e still wrong by up to two orders of magnitude!



J. Wesson, Tokamaks (2004)